C 2

NACA RM E50B23

RESEARCH MEMORANDUM

CALCULATED PERFORMANCE OF NUCLEAR TURBOJET POWERED AIRPLANE AT FLIGHT MACH NUMBER OF 0.9

By Ronald B. Doyle

Lewis Flight Propulsion Laboratory
Cleveland, Ohio

NATIONAL ADVISORY COMMITTEE
FOR AERONAUTICS

WASHINGTON

May 11, 1950
Declassified December 10, 1959

NATIONAL ADVISORY COMMITTEE FOR AERONAUTICS

RESEARCH MEMORANDUM

CALCULATED PERFORMANCE OF NUCLEAR TURBOJET POWERED AIRPLANE AT FLIGHT MACH NUMBER OF 0.9

By Ronald B. Doyle

SUMMARY

An analysis has been made to estimate the performance of a nuclear-energy powered turbojet engine and the optimum engine conditions and to determine the gross weight and the load-carrying capacity of an airplane powered by such an engine. The analysis is for a flight Mach number of 0.9 and covers a range of engine operating conditions and nuclear reactor and reactor-shielding dimensions.

For practical shielding thicknesses, the optimum compressor pressure ratios were high (in the vicinity of 40). The gross weight of the airplane required to carry a disposable load of 20,000 pounds was found to vary from approximately 300,000 to 900,000 pounds, depending on the assumptions. For the case of a reactor tube-wall mean temperature of 2500° R, a turbine-inlet temperature of 2000° R, a reactor free-flow area ratio of 0.33, a reactor-shielding specific gravity of 6.0, a reactor shielding thickness of 3 feet, and an altitude of 30,000 feet, the airplane gross weight required to carry a 20,000-pound pay load was found to be 545,000 pounds.

INTRODUCTION

Because of the possibility of a nearly unlimited flight range inherent in the use of nuclear-powered aircraft, consideration is being given to various types of propulsion system utilizing a nuclear reactor as an energy source. Some aspects of the application of nuclear energy to steam-turbine power plants for aircraft are reported in reference 1.

An analysis was made at the NACA Lewis laboratory of a nuclear-powered turbojet engine over a wide range of conditions. The results of this investigation at a flight Mach number of 0.9

are presented herein. The analysis covers a range of altitudes, reactor-tube-wall temperatures, turbine-inlet temperatures, reactor free-flow-area ratios, compressor pressure ratios, and air mass flows. The investigation is divided into two parts: The first phase of the investigation considers the effects of various operating conditions on the engine performance, and the second considers the gross weight and load-carrying capacity of the complete airplane. Although detailed reactor-design problems are not considered, the analysis shows the effect of several reactor-design variables on the performance of the propulsion system and the aircraft gross weight.

ANALYSIS

Description of Power Plant

A schematic diagram of the turbojet engine, which is conventional except that a nuclear reactor is incorporated in place of the usual combustors, is shown in figure 1. Compression of the air is accomplished in two phases with intercooling between the two axial-flow compressors. The pressure ratio across each of the two compressors is taken equal to the square root of the over-all pressure ratio. The energy addition to the working fluid is accomplished through forced-convection heat transfer from the nuclear-energy-heated passages of the reactor to the air rather than through the combustion of air with fuel as in the conventional turbojet engine. From the reactor, the air passes through a turbine that drives the compressors and finally expands through a nozzle into the atmosphere in the conventional manner. The ratio of the diffuser pressure rise to the compressible dynamic pressure was assumed to be 0.9; the intercooler effectiveness, 50 percent; compressor small-stage efficiency, 88 percent; the adiabatic turbine efficiency, 90 percent; and the velocity coefficient of the exhaust nozzle, 0.96.

Range of Conditions Investigated

Calculations of the performance of this system were made for five combinations of altitude, reactor-tube-wall temperature, turbine-inlet temperature, and reactor free-flow-area ratio for a flight Mach number of 0.9, for a range of compressor pressure ratios from 10 to 50, and for various mass flows per unit reactor frontal area. The following table lists the five sets of conditions investigated:

Altitude, (ft)	Rector tube-wall temperature ($^{\circ}R$)	Turbine-inlet temperature ($^{\circ}R$)	Rector free-flow-area ratio
30,000	2500	2000	0.50
30,000	2500	2000	.33
30,000	2000	1700	.50
30,000	2000	1700	.33
50,000	2500	2000	.50

For each of these conditions the effects of various reactor diameters and shielding thicknesses on the airplane load-carrying capacity and airplane gross weight were investigated.

Method of Calculation

From the momentum equation, the net thrust per slug per second of air is

$$F/M = (V_j - V_0) \tag{1}$$

The definitions of the symbols used throughout this report with the assumed efficiencies and coefficients are given in appendix A. Equation (B4) of appendix B, which is a form of equation (B4) from reference 2, gives the jet velocity, when the effect of reheat due to turbine loss is neglected, as

$$V_j = \sqrt{2C_v^2 J c_{p,t} g T_0 \left(\frac{T_4}{T_0}\right)\left(\frac{T_7}{T_4}\right)\left[1 - \left(\frac{P_0}{P_4}\right)^{\frac{\gamma_t - 1}{\gamma_t}}\left(\frac{P_4}{P_7}\right)^{\frac{\gamma_t - 1}{\gamma_t}}\right] - \frac{1100 C_v^2}{\eta_t}\left(\frac{hp_c}{M}\right)} \tag{2}$$

The magnitude of the error that is introduced by neglecting the effect of reheat depends on the turbine-exit velocity. For the case where the turbine-exit-velocity is equal to the jet velocity, no error is introduced by neglecting the turbine reheat effect. If the turbine-exit velocity is zero, the jet velocities as calculated herein would be about 5 percent lower than those that would be obtained if the effect of reheat were included in the calculation.

For a specified altitude, flight Mach number, compressor pressure ratio, and set of turbojet component efficiencies (ϵ_d, ϵ_i, η_c, η_t, and C_v), the jet velocity as given by equation (2) and hence the net thrust per unit mass flow is a function only of total-temperature and total-pressure ratios T_7/T_4 and P_4/P_7.

Equation (C11) of (appendix C) gives the temperature ratio

$$\frac{T_7}{T_4} = 1 + \left(\frac{T_w}{T_4} - 1\right)\left(1 - e^{-0.00568(l/d)_{eff}}\right) \tag{3}$$

The total-temperature ratio is thus a function of the reactor-tube-wall temperature, the reactor-inlet temperature, and an effective length-to-diameter ratio. For most of the calculations, the tube-wall temperature, reactor-inlet temperature, and the turbine-inlet temperature were specified and equation (3) was used to calculate the effective length-to-diameter ratio, which, as subsequently described, was then used to determine the reactor pressure drop and the actual length-to-diameter ratio of the reactor tubes. The effective length-to-diameter ratio is defined by equation (C8)(appendix C) as follows:

$$\left(\frac{l}{d}\right)_{eff} = 19.22\left(\frac{M}{A_r}\frac{gd}{f\mu_w}\right)^{-0.2}\left(\frac{\rho_w}{\rho_b}\right)^{0.8}\left(\frac{c_{p,w}}{c_{p,b}}\right)\frac{l}{d} \tag{4}$$

From this equation, the effective length-to-diameter ratio is seen to be a function of the tube Reynolds number, the actual length-to-diameter ratio of the reactor tubes, the ratio of air density evaluated at the tube-wall temperature to the air density evaluated at the average air temperature, and the ratio of the specific heat of air evaluated at the tube-wall temperature to the average specific heat.

The assumption of a constant tube-wall temperature was made for the purpose of simplifying the calculations and would be difficult to obtain in an actual reactor. This wall temperature may be considered a mean effective wall temperature for the actual reactor and the maximum wall temperature of a reactor may be appreciably greater than this mean effective wall temperature. The difference between the maximum wall temperature and the mean effective wall temperature can be minimized by the use of neutron reflectors and by adjusting the distribution of fissionable material in the reactor. This subject is not investigated herein.

The pressure drop from station 4 to station 7 (fig. 1) was divided into three parts, a pressure drop from the compressor outlet to the reactor-tube inlet, a pressure drop through the reactor tubes, and a pressure drop from the reactor-tube outlet to the turbine inlet. The pressure drops immediately before (station 4 to 5) and after (station 6 to 7) the reactor tubes were assumed to be approximately equal to $\frac{1}{2}\rho v^2$ as indicated by equations (C12) and (C13) of appendix C. The pressure drop from station 5 to 6 through the reactor tubes was determined by means of the special pressure-drop charts of reference 3. These charts, which are set up for heat transfer to air at a constant wall temperature, yield a solution for the pressure drop in a tube when the wall temperature, the mass flow of air per unit flow area, the effective-length-to-diameter ratio, and the total temperature and pressure at the tube inlet are specified. A complete description of the development and use of these charts is given in reference 3.

The thrust per unit reactor frontal area is the product of the thrust per unit mass flow from equation (1) and the mass flow per unit reactor frontal area. Thus

$$\frac{F}{A_r} = \frac{F}{M}\frac{M}{A_r} \tag{5}$$

The drag of the engine nacelle per unit reactor frontal area from equation (B22) in appendix B is

$$\frac{D_n}{A_r} = \frac{C_d \rho_0 V_0^2}{2g}\frac{M}{A_r}\frac{A_e}{M} \tag{6}$$

The airplane gross weight per unit reactor frontal area is

$$\frac{W_g}{A_r} = \left(\frac{F}{A_r} - \frac{D_n}{A_r}\right)\frac{L}{D} \tag{7}$$

and the ratio of disposable load to gross weight from equation (B27) of appendix B is

$$\frac{W_d}{W_g} = 0.6 - \frac{\frac{W_e}{M}\frac{M_r}{A_r} + \rho_r l(1-f) + \frac{W_{sh}}{A_r}}{\left(\frac{F}{A_r} - \frac{D_n}{A_r}\right)\frac{L}{D}} \tag{8}$$

It was assumed that the reactor and shielding would fall within the frontal area of the compressor or could be submerged in the wings or fuselage of the airplane. The compressor frontal area was therefore used for calculating the nacelle drag and was determined from the air-flow requirements assuming a constant axial Mach number and assuming that the air flow per square foot of compressor frontal area was 25 pounds per second per square foot at sea-level static conditions. This value is approximately the upper limit of the air flow per unit of compressor frontal area handled by current turbojet engines.

The method of calculating engine weights (weight exclusive of reactor, reactor shielding, and intercooler) considered the specific engine weight (lb of engine/lb of air handled) to be a function of the compressor pressure ratio, altitude, and flight speed. The engine weights used in these computations are representative of the lightest of current turbojet engines. Further discussion of the method of evaluating system weight is given in appendix D.

RESULTS AND DISCUSSION

Engine Performance

Thrust per unit reactor frontal area. - The variation of the thrust per unit reactor frontal area F/A_r with the effective length-to-diameter ratio $(l/d)_{eff}$ of the reactor passages is shown in figure 2 for various mass flows per unit reactor frontal area M/A_r. These curves are for an altitude of 30,000 feet, a reactor-tube-wall temperature of 2500° R, a compressor pressure ratio of 40, and a reactor free-flow-area ratio of 0.50.

For constant inlet conditions to the reactor, that is, constant flight Mach number, altitude, compressor pressure ratio, and tube-wall temperature, the turbine-inlet (reactor-outlet) temperature is a function only of effective length-to-diameter ratio. (See equation (3).) A scale of turbine-inlet temperature has been included in figure 2. For a constant effective length-to-diameter ratio and hence constant turbine-inlet temperature, the actual length-to-diameter ratio of the reactor tubes is constant within about 10 percent for the range of mass flow per unit reactor frontal area shown.

As effective length-to-diameter ratio is increased, the turbine-inlet temperature increases with a consequent increase in jet thrust per unit reactor frontal area. At the same time, however, the

pressure drop in the reactor increases because of the increase in passage length-to-diameter ratio and eventually offsets the effect of increasing turbine-inlet temperature so that the thrust begins to decrease. The point of maximum thrust per unit reactor frontal area occurs at progressively higher effective length-to-diameter ratios and turbine-inlet temperatures as the mass flow per unit reactor frontal area decreases. The maximum points for the curves of mass flow per unit reactor frontal area of 4.0 and 4.5 slugs per second per square foot occur at effective length-to-diameter ratios corresponding to a tube-outlet Mach number of 0.65.

The calculations for the remainder of the figures were made for constant turbine-inlet temperatures of either 2000° or 1700° R. A cross plot from figure 2 of thrust per unit reactor frontal area F/A_r against mass flow permit reactor frontal area M/A_r at a turbine-inlet temperature of 2000° R is shown in figure 3 along with similar curves for other compressor pressure ratios P_4/P_1.

For a constant compressor pressure ratio, increasing the mass flow per unit reactor frontal area increases the jet thrust because the engine is handling more air at the same conditions of temperature and pressure. As the length-to-diameter ratio of the reactor tubes is essentially constant (for a constant turbine-inlet temperature), however, the pressure drop also increases with mass flow per unit reactor frontal area and eventually causes the thrust per unit area to decrease.

The maximum points of thrust per unit reactor frontal area F/A_r at each pressure ratio are plotted against compressor pressure ratio P_4/P_1 in figure 4 together with similar curves for the other conditions of altitude, tube-wall temperature, turbine-inlet temperature, and reactor free-flow-area ratio investigated in this analysis.

As the compressor pressure ratio is initially increased, the thrust per unit reactor frontal area increases because the optimum values of mass flow per unit reactor frontal area are increasing, as indicated in figure 3. The thrust finally decreases, however, with increasing compressor pressure ratio because of the effects of the limiting turbine-inlet temperature also found with the conventional turbojet engine. Maximum thrust per unit area appears to occur at a compressor pressure ratio slightly higher than 50 for the conditions where the tube-wall temperature is 2500° R and the turbine-inlet temperature is 2000° R (fig. 4). The curves for a tube-wall temperature of 2000° R and a turbine-inlet temperature of 1700° R have their maximum thrust per unit area at a compressor pressure ratio of about 30.

Reducing the free-flow area ratio from 0.50 to 0.33 at an altitude of 30,000 feet, a tube-wall temperature of 2500° R, a turbine-inlet temperature of 2000° R, and a compressor pressure ratio of 50 results in about a 35-percent decrease in thrust per unit reactor frontal area. A change in altitude from 30,000 to 50,000 feet causes a reduction in thrust per unit reactor frontal area of about 53 percent. (Compare top curve of fig. 4 with solid curve.)

The maximum thrust for the condition where the tube-wall temperature is 2000° R, the turbine-inlet temperature is 1700° R and the free-flow area ratio is 0.50 is approximately 58 percent lower than the maximum thrust for the top curve (tube-wall temperature, 2500° R; turbine-inlet temperature, 2000° R). Comparison of the top curve with the dotted curve shows the combined effect of reducing the free-flow area ratio from 0.50 to 0.33, the tube-wall temperature from 2500° to 2000° R, and the turbine-inlet temperature from 2000° to 1700° R.

Thrust and net thrust per unit engine frontal area. - The variation of the thrust and the net thrust (thrust less engine-nacelle drag) per unit of engine frontal area, F/A_e and $(F-D_n)/A_e$, respectively, with mass flow per unit reactor frontal area M/A_r for various compressor pressure ratios P_4/P_1 is shown in figure 5. The engine frontal area is based on the frontal area of the compressor. The altitude is 30,000 feet, the tube-wall temperature, 2500° R, the turbine-inlet temperature, 2000° R, and the reactor free-flow-area ratio, 0.50. These curves also indicate the variation of thrust per unit mass flow because for a given flight speed and altitude the air mass flow per unit engine frontal area is constant.

As the mass flow per unit reactor frontal area is increased at a constant compressor pressure ratio, the reactor pressure drop increases with a consequent decrease in thrust per unit mass flow of air and thrust per unit engine frontal area. The slope of a line drawn from the origin in figure 3 to any point on a curve gives the value of the thrust per unit mass flow, which for a given flight condition is proportional to the thrust per unit engine frontal area for that point. It is hence apparent from figure 3 that the thrust per unit mass flow and thrust per unit engine frontal area decrease as mass flow per unit reactor frontal area increases. For the range of compressor pressure ratios investigated, the thrust per unit engine frontal area decreases with increasing compressor pressure ratio. This effect is a reflection of the decrease in thrust per unit mass flow that occurs

beyond the optimum compressor pressure ratio for conventional turbojet-engine cycles. The dashed curves of net thrust per unit engine frontal area show the same trend and are lower by the amount of the constant nacelle drag per unit engine frontal area.

The net thrusts per unit engine frontal area shown in figure 5 may be somewhat higher than those for a conventional turbojet engine because $(F-D_n)/A_e$ is based on the compressor frontal area rather than on the slightly larger combustor frontal area, which is used for most turbojet-engine calculations.

Specific thrust. - The variation of the net thrust (thrust minus nacelle drag) per unit of engine weight plus reactor weight $(F-D_n)/(W_e+W_r)$ with mass flow per unit reactor frontal area M/A_r for a reactor length of 2 feet and for various compressor pressure ratios for the case of an unshielded reactor is shown in figure 6. Subsequent curves show the specific thrust including various amounts of reactor-shielding weight.

For a constant compressor pressure ratio, the thrust per unit of engine weight plus reactor weight varies in nearly the same manner as the thrust per unit engine frontal area because, as previously mentioned, the engine weight per unit engine frontal area is a constant for each compressor pressure ratio (the reactor weight being only a small percentage of the engine weight).

The thrust per unit engine weight decreases more rapidly with increasing compressor pressure ratio than the thrust per unit engine frontal area because of increasing engine weight per unit engine frontal area.

For a constant compressor pressure ratio, mass flow per unit reactor frontal area, altitude, tube-wall temperature, and turbine-inlet temperature, the specific thrust decreases with decreasing free-flow-area ratio because of the increasing reactor pressure drop.

The decrease in specific thrust with decreased tube-wall and turbine-inlet temperature is due mainly to a decrease in thrust per unit mass flow of air because of the reduced temperature at the nozzle inlet.

Other conditions being constant, the specific thrust decreases as the altitude is increased from 30,000 to 50,000 feet because at the higher altitude a larger engine is required to handle a given amount of air.

The variation of the net thrust per unit of power-plant weight $(F-D_n)/(W_e+W_r+W_{sh})$ with mass flow per unit reactor frontal area M/A_r for various compressor pressure ratios and specified values of shielding weight per unit of reactor frontal area W_{sh}/A_r is shown in figure 7.

For a constant compressor pressure ratio and shielding weight per unit reactor frontal area, the specific thrust increases to a maximum value and then decreases as the mass flow per unit reactor frontal area increases. The large constant value of shielding weight per unit reactor frontal area along each of the curves in figure 7 tends to minimize the effect of the increasing system weight and accents the effect of the increasing thrust per unit reactor frontal area. As M/A_r continues to increase, however, the increasing engine weight eventually becomes of sufficient importance to cause the specific thrust to decrease.

In figure 8 the maximum points from figure 7 and from similar plots for the other four general conditions are plotted against compressor pressure ratio P_4/P_1 for various shielding weights per unit reactor frontal area W_{sh}/A_r. In figure 6, the specific thrust of a system with a bare reactor (zero shielding weight) was observed to decrease with increased compressor pressure ratio, for the range investigated, because of an increase in engine weight that offset the effect of increasing net thrust. Because shielding the reactor, however, tends to lessen the importance of the increasing engine weight (that is, the percentage increase in total system weight is less in this case), there is an initial increase in specific thrust with increasing compressor pressure ratio. Eventually, however, the engine weight increases at a sufficiently rapid rate to cause the specific thrust to decrease with increasing compressor pressure ratio.

The compressor pressure ratio for maximum specific thrust increases as the shielding weight per unit reactor frontal area, and tube-wall and turbine-inlet temperatures increase (fig. 8). The compressor pressure ratio for maximum specific thrust varies also with altitude and reactor free-flow-area ratio. For a tube-wall temperature of 2500° R and a turbine-inlet temperature of 2000° R (figs. 8(a), 8(b), and 8(e)), the compressor pressure ratio for maximum specific thrust varies from below 10 for the unshielded case (see fig. 6) to about 35 at a shielding weight per unit reactor frontal area of 10,000 pounds per square foot and to about 48 at a shielding weight per unit reactor frontal area of 50,000 pounds per

square foot. For a tube-wall temperature of 2000° R and a turbine-inlet temperature of 1700° R (figs. 8(c) and 8(d)), optimum compressor pressure ratio varies from about 20 at a shielding weight per reactor frontal area of 10,000 pounds per square foot to about 25 at a shielding weight per reactor frontal area of 50,000 pounds per square foot.

The previously mentioned effects of varying altitude, tube-wall and turbine-inlet temperature, and reactor free-flow-area ratio that were mentioned in the discussion of figure 6 also apply to figure 8.

The shielding weight per unit reactor frontal area, which was included as a parameter in figure 8, is for a cylindrical reactor a function of the shielding thickness, the reactor diameter, the reactor length, and the specific gravity of the shielding material. Figure 9 shows for a cylindrical reactor the variation of the shielding weight per unit reactor frontal area W_{sh}/A_r with shielding thickness t_{sh} for various reactor diameters d_r and lengths l and for a specific gravity of the shielding material of 6.0. The calculations for the shielding weights shown in figure 9 and subsequent figures are based on a simple configuration of a constant shielding thickness around a cylindrical reactor and do not take into account the weight of the shielding around the air ducts to and from the reactor. The weight of shielding necessary for this additional shielding would largely depend on the ducting arrangement. For a cylindrical reactor 4 feet in diameter and 4 feet long and a shielding thickness of 3 feet, one preliminary ducting layout and weight analysis indicated that, for a duct flow area equal to the reactor flow area, the ducted shielding would weigh about 25 percent more than the simple shielding arrangement assumed in this analysis. This percentage increase in weight would be expected to vary somewhat with reactor and shielding dimensions.

The shielding weight per unit reactor frontal area increases with increasing shielding thickness and reactor length. For a constant shielding thickness and reactor length, however, the shielding weight per reactor frontal area decreases with increasing reactor diameter because that portion of the shielding weight around the circumference of the reactor increases approximately as the first power of the reactor diameter, whereas the reactor frontal area increases as the diameter squared. Because considerations of economy of fissionable material have an important bearing on the choice of the reactor proportions, no attempt is made herein to indicate optimum proportions. Other coolant-passage arrangements may make possible some reduction in shielding weight for a given rate of reactor power output.

Airplane Gross Weight and Load-Carrying Capacity

Disposable-load-to-gross-weight ratio. - Figure 10 shows the variation of the ratio of disposable load to airplane gross weight W_d/W_g with mass flow per unit reactor frontal area M/A_r for various compressor pressure ratios P_4/P_1, reactor diameters d_r, and reactor lengths l and for a shielding thickness of 2 feet. These curves are for an altitude of 30,000 feet, a tube-wall temperature of 2500° R, a turbine-inlet temperature of 2000° R, a reactor free-flow-area ratio of 0.50, a shielding specific gravity of 6.0, and a lift-drag ratio of the airplane without nacelles of 18.

For a constant reactor diameter and length, the ratio of disposable load to gross weight has a maximum value with both flow per unit reactor frontal area and compressor pressure ratio just as the specific-thrust curves of figure 7 because ratio of disposable load to gross weight is a function only of the specific thrust for a constant lift-drag ratio of the airplane, as indicated by equation (8).

For a constant compressor pressure ratio, mass flow per unit reactor frontal area, and reactor length, increasing the reactor diameter results in an increase in the ratio of dispoable load to gross weight because, as indicated in the discussion of figure 9, an increase in reactor diameter results in a decrease in the shielding weight per unit reactor frontal area, whereas the thrust increases in direct proportion to the reactor frontal area or to the square of the reactor diameter. For example: for a constant reactor length of 2 feet, increasing the reactor diameter from 2 to 4 feet increases the reactor frontal area, the air flow, the thrust, and the engine weight by a factor of 4. For a constant shielding thickness of 2 feet, however, this increase in diameter increases the shielding weight by a factor of only 1.8 so that a larger percentage of the airplane gross weight can be carried as disposable load.

Comparison of the top three families of curves in figure 10 shows the effect of varying reactor length with a constant reactor diameter. As the reactor length increases, the ratio of disposable load to gross weight decreases because of a direct increase in the shielding weight. The minimum length reactor that could be used with this power plant is determined by nuclear considerations or by the minimum reactor-passage diameter that is practical, because for a given turbine-inlet temperature, compressor pressure ratio, and tube Reynolds number, the length-to-diameter ratio of the reactor passages is constant. Calculations indicate that for the conditions

of figure 10 and for the range of mass flow per unit reactor frontal area and compressor pressure ratios investigated, the tube diameter varies from 0.18 to 0.21 inch for a reactor length of 2 feet, from 0.26 to 0.30 inch for a reactor length of 3 feet, and from 0.34 to 0.38 inch for a reactor length of 4 feet. It is again emphasized that these conclusions apply for the simple reactor flow-passage arrangement assumed in the analysis.

The changes in ratio of disposable load to gross weight shown in figure 10 are accompanied by variations in the airplane gross weight because the gross weight is a function of the net thrust and hence mass flow per unit reactor frontal area, compressor pressure ratio, and reactor diameter. The gross weight is independent of the reactor length for the assumptions of the present analysis. A plot of the gross weights, corresponding to the disposable-load-to-gross-weight ratios W_d/W_g of figure 10, against mass flow per unit reactor frontal area M/A_r is shown in figure 11. The corresponding ranges of values of ratio of disposable load to gross weight for a reactor length of 2 feet are also presented. For a constant reactor diameter, the variation in gross weight shown by these curves is a direct result of the variation of net thrust per unit reactor frontal area. For a given mass flow per unit reactor frontal area and compressor pressure ratio, the net thrust and hence the gross weight are directly proportional to the square of the reactor diameter.

The maximum values of disposable-load-to-gross-weight ratio W_d/W_g (at optimum compressor pressure ratio and mass flow per unit reactor frontal area) from figure 10 and from similar plots for the other conditions are plotted against the corresponding gross weights W_g in figure 12. In addition to the five general conditions for which curves are presented throughout this report, figure 12 includes curves for a set of conditions at an altitude of 70,000 feet, a tube-wall temperature of 2500° R, a turbine-inlet temperature of 2000° R, and a reactor free-flow-area ratio of 0.50 (fig. 12(f)).

The curves are for a reactor length of 2 feet, a specific gravity of the shielding material of 6.0, and a lift-drag ratio of the airplane without nacelles of 18. A line for a constant disposable load of 20,000 pounds is also shown. Similar lines for other values of disposable load can readily be plotted on this figure.

As previously mentioned in the discussion of figures 10 and 11, increasing the reactor diameter with a constant shielding thickness results in an increase in ratio of disposable load to gross weight and in the airplane gross weight. For a constant reactor diameter, increasing the shielding thickness decreases the ratio of disposable load to gross weight and increases the gross weight.

For an altitude of 30,000 feet, a tube-wall temperature of 2500° R, a turbine-inlet temperature of 2000° R, a reactor free-flow area ratio of 0.50, a disposable load of 20,000 pounds, and shielding thickness of 3.5 feet, the required airplane gross weight would be about 680,000 pounds (fig. 12(a)). For the same conditions and a shielding thickness of 3 feet, an airplane weighing about 450,000 pounds would be required.

Inspection of figure 12(f), which is for an altitude of 70,000 feet, indicates that for the range of shielding thicknesses and reactor diameters investigated the values of the ratio of disposable load to gross weight are for the most part negative. When this ratio is negative, the airplane will not fly at the specified conditions. For example, for reactor diameters up to 10 feet the airplane will not fly with 1.5 feet of reactor shielding. For a reactor diameter of 10 feet and a shielding thickness of about 1.25 feet an airplane weighing about 475,000 pounds will fly but can carry no disposable load. If the airplane is to carry a disposable load of 20,000 pounds and the reactor diameter is to be 10 feet, the maximum shielding thickness that can be allowed is about 1.1 feet and the airplane gross weight would be 355,000 pounds. More favorable assumptions for either the engine or the airplane would increase the disposable-load-to-gross-weight ratios or for a fixed disposable load would decrease the airplane gross weights required. For example, the assumption that the structural weight of the airplane was 30 percent of the airplane gross weight, rather than the value of 40 percent used in this analysis, would raise all the curves of figure 12 by 0.1 on the W_d/W_g scale. Further comparison of figures 12(a) to 12(e) will be made in a subsequent table.

As previously mentioned, the shielding weights and the shielding thickness as calculated herein do not include the shielding around the air ducting to and from the reactor so that the disposable-load-to-gross-weight ratios and the required airplane gross weights shown here are somewhat optimistic for the shielding thicknesses given. The previously mentioned 25-percent increase in shielding weight that is necessary to allow for the duct shielding is equivalent to a 10- to 15-percent increase in shielding thickness for thicknesses of

about 3 feet. The additional shielding thickness required for ducting can thus be taken into consideration in the curves of figure 12 for shielding thicknesses of about 3 feet by increasing the values shown by 10 to 15 percent.

A considerable decrease in required airplane gross weight can be realized if equal shielding ability can be obtained by reducing the shielding thickness and increasing the specific gravity of the shielding material to maintain a constant product of the two quantities. The following table shows, for a disposable load of 20,000 pounds and for the conditions of figure 12(a), the decrease in airplane gross weight that can be realized by reducing the shielding thickness and maintaining the product of specific gravity and shielding thickness constant at 18:

Specific gravity of shielding material	Shielding thickness (ft)	Reactor diameter (ft)	Airplane gross weight (lbs)
6	3.0	2.7	450,000
9	2.0	2.2	260,000
12	1.5	1.9	180,000

Any reduction in shielding weight that results from improvement in shielding methods will make the application of the nuclear-energy power plant more feasible than shown in this analysis.

The selection of values of turbine-inlet temperature used in this analysis were based on the material limitations in the turbine. Somewhat lower required airplane gross weights than those shown in figure 12 could be obtained if the calculations were made for the optimum turbine-inlet temperatures.

Optimum compressor pressure ratio. - The compressor pressure ratios P_4/P_1 for maximum ratio of disposable load to gross weight W_d/W_g corresponding to the values of the ratio of disposable load to gross weight in figure 12 are plotted in figure 13 against the reactor-shielding thickness t_{sh} for the various reactor diameters and for the five general conditions investigated. In each case, the optimum compressor pressure ratio increases with increasing shielding thickness and decreasing reactor diameter. The optimum compressor pressure ratio decreases with a decrease in tube-wall and turbine-inlet temperature.

Reactor output. - The reactor outputs Q_r corresponding to the curves of ratio of disposable load to gross weight in figure 12 are shown plotted against the reactor-shielding thickness t_{sh} for various reactor diameters in figure 14. The reactor output increases with both shielding thickness and reactor diameter for all the conditions investigated.

The following table gives the required airplane gross weights and reactor diameters along with the corresponding optimum compressor pressure ratios, engine thrusts, and reactor outputs as obtained from figures 12 to 14 for various operating conditons and for a disposable load of 20,000 pounds.

Altitude (ft)	Reactor tube-wall temperature (°R)	Turbine-inlet temperature (°R)	Reactor free-flow-area ratio	Reactor-shielding thickness[1] (ft)	Reactor diameter[2] (ft)	Optimum compressor pressure ratio	Engine thrust (lb)	Reactor output (Btu/sec)	Airplane gross weight (lb)
30,000	2500	2000	0.50	2.5	2.2	39	16,500	91,000	275,000
30,000	2500	2000	.33	2.5	3.0	39	19,500	106,000	325,000
30,000	2000	1700	.50	2.5	4.0	24	23,300	130,000	375,000
30,000	2000	1700	.33	2.5	5.7	22	32,800	185,000	530,000
50,000	2500	2000	.50	2.5	5.2	35	38,200	208,000	650,000
30,000	2500	2000	.50	3.0	2.7	40	26,900	140,000	450,000
30,000	2500	2000	.33	3.0	3.8	40	32,500	180,000	545,000
30,000	2000	1700	.50	3.0	5.1	24	39,600	260,000	640,000
30,000	2000	1700	.33	3.0	7.6	23	56,700	375,000	915,000

[1]Specific gravity of shielding, 6.0.

[2]Reactor length, 2.0 ft.

Comparison of the first line of the table with each succeeding line shows in turn, the effect on airplane gross weight and the reactor output of changes in (a) free-flow-area ratio, (b) tube-wall and turbine-inlet temperature, (c) tube-wall temperature, turbine-inlet temperature, and free-flow area ratio, and (d) altitude. For a fixed disposable load a reduction in tube-wall temperature, turbine-inlet temperature, or free-flow area ratio, or an increase in altitude increased the required airplane gross weight, the reactor output, and the engine thrust.

Maximum allowable shielding thickness for a fixed disposable load. - The variation of the maximum allowable shielding thickness with airplane gross weight W_g for various reactor diameters and airplane lift-drag ratios (lift-drag ratios without nacelles) and a disposable load of 20,000 pounds is shown in figure 15. The mass flow per unit reactor frontal area and the compressor pressure ratio are the optimum values for maximum shielding thickness with minimum airplane gross weight. The curves are for an altitude of 30,000 feet, a tube-wall temperature of 2500° R, a turbine-inlet temperature of 2000° R, a reactor free-flow-area ratio of 0.50, a specific gravity of shielding material of 6.0, and a reactor length of 2 feet.

For a constant lift-drag ratio, the allowable shielding thickness increases at a diminishing rate as the gross weight of the airplane and the corresponding reactor diameter increase. For a reactor diameter of 3 feet, an airplane with a lift-drag ratio of 18 can carry 3.2 feet of reactor shielding along with the disposable load of 20,000 pounds, and the gross weight would be about 510,000 pounds. Increasing the reactor diameter to 4 feet increases the allowable shielding thickness to about 3.9 feet and the gross weight to 900,000 pounds. A decrease in the lift-drag ratio from 20 to 14 for the 3-foot diameter reactor reduces the allowable shielding thickness from 3.4 to 2.7 feet and the gross weight from 560,000 to 400,000 pounds.

SUMMARY OF RESULTS

The results of calculations on the performance of a nuclear turbojet-powered airplane may be summarized as follows:

1. The compressor pressure ratio for maximum specific thrust and maximum ratio of disposable load to airplane gross weight (a measure of load-carrying capacity of the airplane) increased as the shielding weight or turbine-inlet temperature increased. The optimum compressor pressure ratio also varied with altitude and reactor free-flow-area ratio. For each compressor pressure ratio, there was a corresponding optimum mass flow per unit reactor frontal area, which was determined by the pressure drop in the reactor passages.

2. A reduction in tube-wall temperature, turbine-inlet temperature, or free-flow-area ratio, or an increase in altitude decreased the ratio of disposable load to gross weight or, for a fixed disposable load, increased the required airplane gross weight.

3. For a constant shielding thickness and reactor length, increasing the reactor diameter increased the disposable-load-to-gross-weight ratio and the gross weight. For a constant reactor diameter, an increase in shielding thickness or reactor length resulted in a decrease in disposable-load-to-gross-weight ratio.

4. The following table gives the required airplane gross weights and reactor diameters, along with the corresponding optimum compressor pressure ratios, engine thrust, and reactor outputs for various operating conditions and for a disposable load of 20,000 pounds:

Altitude (ft)	Reactor tube-wall temperature (°R)	Turbine-inlet temperature (°R)	Reactor free-flow-area ratio	Reactor-shielding thickness[1] (ft)	Reactor diameter[2] (ft)	Optimum compressor pressure ratio	Engine thrust (lb)	Reactor output (Btu/sec)	Airplane gross weight (lb)
30,000	2500	2000	0.50	2.5	2.2	39	16,500	91,000	275,000
30,000	2500	2000	.33	2.5	3.0	39	19,500	106,000	325,000
30,000	2000	1700	.50	2.5	4.0	24	23,300	130,000	375,000
30,000	2000	1700	.33	2.5	5.7	22	32,800	185,000	530,000
50,000	2500	2000	.50	2.5	5.2	35	38,200	208,000	650,000
30,000	2500	2000	.50	3.0	2.7	40	26,900	140,000	450,000
30,000	2500	2000	.33	3.0	3.8	40	32,500	180,000	545,000
30,000	2000	1700	.50	3.0	5.1	24	39,600	260,000	640,000
30,000	2000	1700	.33	3.0	7.6	23	56,700	375,000	915,000

[1]Specific gravity of shielding, 6.0.

[2]Reactor length, 2.0 ft.

Lewis Flight Propulsion Laboratory,
National Advisory Committee for Aeronautics,
Cleveland, Ohio, July 7, 1949.

APPENDIX A

SYMBOLS

The following symbols are used in this report:

A_e	turbojet engine frontal area, sq ft
A_f	reactor-tube (flow) area, sq ft
A_r	reactor frontal area, sq ft
C_D	drag coefficient of engine nacelle (assumed to be 0.09)
C_v	velocity coefficient of discharge nozzle (assumed to be 0.96)
$c_{p,b}$	specific heat at constant pressure of air in reactor tubes evaluated at average air temperature, Btu/(lb)/($^{\circ}$F)
$c_{p,c}$	specific heat at constant pressure of air in compressor, Btu/(lb)/($^{\circ}$F) (average value of 0.2436 used)
$c_{p,t}$	specific heat at constant pressure of air in turbine, Btu/(lb)/($^{\circ}$F) (average value of 0.2644 used)
$c_{p,w}$	specific heat at constant pressure of air in reactor tubes evaluated at tube-wall temperature, Btu/(lb)/($^{\circ}$F)
D_n	profile drag of engine nacelle, lb
d	diameter of reactor tubes, ft
d_r	diameter of reactor, ft
F	thrust of turbojet engine, lb
f	reactor free-flow-area ratio, A_f/A_r
g	acceleration due to gravity, 32.2 ft/sec^2
h	coefficient of heat transfer, Btu/(sec)(sq ft)($^{\circ}$F)
hp_c	compressor power, hp

hp_t	turbine power, hp
J	mechanical equivalent of heat, 778 ft-lb/Btu
k_w	thermal conductivity of air in reactor tubes evaluated at tube-wall temperature, Btu/(sec)(ft)(^oF)
L/D	lift-drag ratio of airplane without nacelles
l	length of reactor or reactor tubes, ft
$(l/d)_{eff}$	effective length-to-diameter ratio of reactor tubes as defined by equation (C8) (appendix C)
M	mass flow of air, slugs/sec
P	total pressure, lb/sq ft absolute
ΔP	total-pressure drop, lb/sq ft
p	static pressure, lb/sq ft absolute
Q	heat transferred, Btu/sec
Q_r	reactor energy output, Btu/sec
R	gas constant for air, 53.35 ft-lb/(lb)(^oF)
S	inside tube surface area, sq ft
s	inside tube surface area per unit length, sq ft/ft
T	total temperature, ^oR
T_w	mean effective temperature of reactor passage walls, ^oR
t	static temperature, ^oR
t_{sh}	reactor shielding thickness, ft
V_j	jet velocity, ft/sec
V_o	flight velocity, ft/sec
v	velocity of air, ft/sec

W_d	disposable load, $W_d = W_g - W_{st} - W_e - W_{sh} - W_r$, lb
W_e	weight of engine excluding reactor and shielding weights, lb
W_g	gross weight of airplane, lb
W_r	weight of reactor, lb
W_{sh}	weight of reactor shielding, lb
W_{st}	structural weight of airplane, lb (assumed to be 0.4 W_g)
W/A_e	air flow per unit engine frontal area at any conditions, lb/(sec)(sq ft)
$(W/A_e)_s$	air flow per unit engine frontal area at standard conditions (pressure 2116.4 lb/sq ft and temperature 518° R), lb/(sec) (sq ft) (value of 25 used)
γ_c	ratio of specific heats of air in compressor (average value of 1.392 used)
γ_t	ratio of specific heats of air in turbine (average value of 1.350 used)
ϵ_d	diffuser pressure-rise recovery factor (assumed to be 0.90)
ϵ_i	intercooler effectiveness (assumed to be 0.50)
η_c	compressor small-stage efficiency (assumed to be 0.88)
η_t	adiabatic turbine efficiency (assumed to be 0.90)
μ_w	viscosity of air in reactor tubes evaluated at tube-wall temperature, lb/ft-sec
ρ	density of air, lb/cu ft
ρ_b	density of air in tubes evaluated at average air temperature, lb/cu ft
ρ_r	density of reactor material, lb/cu ft
ρ_w	density of air in reactor tubes evaluated at tube-wall temperature, lb/cu ft

ρ_0 density of ambient air, lb/cu ft

Subscripts:

0	ambient conditions at any altitude
1	compressor inlet
2	intercooler inlet
3	intercooler outlet
4	compressor outlet (reactor inlet)
5	reactor-tube inlet
6	reactor-tube outlet
7	turbine inlet (reactor outlet)

APPENDIX B

JET VELOCITY, THRUST, AND AIRPLANE PERFORMANCE

Jet Velocity and Thrust

From the momentum equation, the net thrust per slug per second of air is

$$F/M = V_j - V_0 \tag{B1}$$

When the effect of reheat due to turbine loss is neglected, the jet velocity is given by equation (B4) from reference 2, thus

$$V_j = C_v\sqrt{2Jc_{p,t}gT_7\left[1 - \left(\frac{p_0}{P_7}\right)^{\frac{\gamma_t-1}{\gamma_t}}\right] - \frac{1100\ hp_t}{M\eta_t(1 + f/a)}} \tag{B2}$$

where f/a is the fuel-air ratio and is equal to zero for this system. Only enough turbine power is removed to drive the compressor, so that

$$hp_t = hp_c \tag{B3}$$

Substituting equation (B3) in equation (B2) and rearranging give

$$V_j = \sqrt{2C_v^2Jc_{p,t}gt_0\left(\frac{T_4}{t_0}\right)\left(\frac{T_7}{T_4}\right)\left[1 - \left(\frac{p_0}{P_4}\right)^{\frac{\gamma_t-1}{\gamma_t}}\left(\frac{P_4}{P_7}\right)^{\frac{\gamma_t-1}{\gamma_t}}\right] - \frac{1100\ C_v^2}{\eta_t}\left(\frac{hp_c}{M}\right)} \tag{B4}$$

The ambient temperature and pressure t_0 and p_0 were obtained from the NACA standard atmosphere tables (reference 4).

The compression power per unit mass flow of air hp_c/M is the sum of the compression power of the two compressors, the one before and the one after the intercooler; thus,

$$\frac{hp_c}{M} = \frac{Jgc_{p,c}}{550}\left[(T_2-T_1)+(T_4-T_3)\right] \tag{B5}$$

$$\frac{hp_c}{M} = \frac{Jgc_{p,c}}{550}\left\{T_1\left[\left(\frac{P_2}{P_1}\right)^{\frac{\gamma_c-1}{\gamma_c\eta_c}}-1\right]+T_3\left[\left(\frac{P_4}{P_3}\right)^{\frac{\gamma_c-1}{\gamma_c\eta_c}}-1\right]\right\} \tag{B6}$$

It was assumed that the intercooling takes place halfway through the compression process so that

$$\frac{P_2}{P_1} = \frac{P_4}{P_3} = \left(\frac{P_4}{P_1}\right)^{\frac{1}{2}} \tag{B7}$$

Then from the definition of cooling effectiveness,

$$T_3 = (1-\epsilon_i)T_2 + \epsilon_i T_1 \tag{B8}$$

and from the definition of small-stage efficiency and the assumed division of compressor work

$$T_2 = T_1\left(\frac{P_4}{P_1}\right)^{\frac{\gamma_c-1}{2\gamma_c\eta_c}} \tag{B9}$$

Therefore

$$T_3 = T_1\left[(1-\epsilon_i)\left(\frac{P_4}{P_1}\right)^{\frac{\gamma_c-1}{2\gamma_c\eta_c}}+\epsilon_i\right] \tag{B10}$$

Substituting equations (B7) and (B10) in equation (B6) gives

$$\frac{hp_c}{M} = \frac{Jgc_{p,c}t_0}{550}\left(\frac{T_1}{t_0}\right)\left[\left(\frac{P_4}{P_1}\right)^{\frac{\gamma_c-1}{2\gamma_c\eta_c}} - 1\right]\left[1 + (1-\epsilon_i)\left(\frac{P_4}{P_1}\right)^{\frac{\gamma_c-1}{2\gamma_c\eta_c}} + \epsilon_i\right] \tag{B11}$$

With the assumption that the square of the velocity at the diffuser outlet is much less than V_0^2, the temperature ratio T_1/t_0 is

$$\frac{T_1}{t_0} = 1 + \frac{V_0^2}{2gJc_{p,c}t_0} \tag{B12}$$

The compressor power per unit mass flow of air is thus a function of the altitude, flight speed, compressor pressure ratio, compressor efficiency, and the intercooler effectiveness. The total-pressure ratio P_1/p_0 was obtained from the definition of the diffuser pressure-rise recovery factor; thus,

$$\frac{P_1}{p_0} = 1 + \epsilon_d\left[\left(1 + \frac{V_0^2}{2gJc_{p,c}t_0}\right)^{\frac{\gamma_c}{\gamma_c-1}} - 1\right] \tag{B13}$$

The total temperature at the reactor inlet is

$$T_4 = T_1 + (T_2-T_1) + (T_4-T_3) - (T_2-T_3) \tag{B14}$$

Equation (B8) may be rearranged to give the temperature drop of the working air in the intercooler. Thus,

$$T_2 - T_3 = \epsilon_i(T_2-T_1) \tag{B15}$$

Also from equation (B9)

$$T_2 - T_1 = T_1\left[\left(\frac{P_4}{P_1}\right)^{\frac{\gamma_c-1}{2\gamma_c\eta_c}} - 1\right] \tag{B16}$$

Therefore,

$$T_2-T_3 = \epsilon_i T_1 \left[\left(\frac{P_4}{P_1} \right)^{\frac{\gamma_c-1}{2\gamma_c\eta_c}} - 1 \right] \tag{B17}$$

The temperature rise across the second compressor is

$$T_4-T_3 = T_3 \left[\left(\frac{P_4}{P_1} \right)^{\frac{\gamma_c-1}{2\gamma_c\eta_c}} - 1 \right] \tag{B18}$$

Substituting the value of T_3 from equation (B10) in equation (B18) gives

$$T_4-T_3 = T_1 \left[(1-\epsilon_i) \left(\frac{P_4}{P_1} \right)^{\frac{\gamma_c-1}{2\gamma_c\eta_c}} + \epsilon_i \right] \left[\left(\frac{P_4}{P_1} \right)^{\frac{\gamma_c-1}{2\gamma_c\eta_c}} - 1 \right] \tag{B19}$$

Substituting equation (B16), (B17), and (B19) in equation (B14) and dividing by T_1 give

$$\frac{T_4}{T_1} = 1 + \left[\left(\frac{P_4}{P_1} \right)^{\frac{\gamma_c-1}{2\gamma_c\eta_c}} - 1 \right] \left[(1-\epsilon_i) \left(\frac{P_4}{P_1} \right)^{\frac{\gamma_c-1}{2\gamma_c\eta_c}} + 1 \right] \tag{B20}$$

The temperature ratio across the compressor is thus a function of compressor pressure ratio, compressor efficiency, and intercooler effectiveness.

The temperature ratio T_4/t_0, which appears in equation (B4) is then the product of T_1/t_0 from equation (B12) and T_4/T_1 from equation (B20). The pressure ratio P_4/p_0 in equation (B4) is the product of the over-all compressor pressure ratio P_4/P_1 and P_1/p_0 from equation (B13).

The jet velocity, as given by equation (B4), and hence the thrust per unit mass flow, is thus seen to be a function only of the total-temperature ratio T_7/T_4 and total-pressure ratio P_7/P_4 across the reactor for a specified flight speed, altitude, compressor pressure ratio, and turbojet component efficiencies (ϵ_d, ϵ_i, η_c, η_t, and C_v).

Airplane and Engine Performance

The thrust per unit reactor frontal area is the product of the thrust per unit mass flow from equation (B1) and the mass flow per unit reactor frontal area, thus

$$\frac{F}{A_r} = \frac{F}{M}\frac{M}{A_r} \tag{B21}$$

The frontal area of the power-plant nacelle was assumed to be equal to the engine frontal area, which was determined from the compressor air handling capacity, as described in appendix D. In view of the uncertainty of the actual installation arrangement, it was further assumed that the reactor and the shielding could be submerged in the engine nacelle or in the airplane fuselage. The drag of the nacelle per unit reactor frontal area is therefore

$$\frac{D_n}{A_r} = \frac{C_D \rho_0 V_0^2}{2g}\frac{M}{A_r}\frac{A_e}{M} \tag{B22}$$

For a given flight speed and altitude, the drag per unit reactor area is thus a function only of the mass flow per unit reactor frontal area and a constant mass flow per unit engine frontal area.

The engine and reactor weights per unit reactor frontal area are

$$\frac{W_e}{A_r} = \frac{W_e}{M}\frac{M}{A_r} \tag{B23}$$

$$\frac{W_r}{A_r} = \rho_r l(1-f) \tag{B24}$$

The engine weight per unit mass flow of air W_e/M was assumed to be a function only of flight conditions and compressor pressure ratio, as described in appendix D.

The gross weight of the airplane per unit reactor frontal area is given by the equation

$$\frac{W_g}{A_r} = \left(\frac{F}{A_r} - \frac{D_n}{A_r}\right)\frac{L}{D} \tag{B25}$$

and the disposable load per unit reactor frontal area by

$$\frac{W_d}{A_r} = \frac{W_g}{A_r} - \frac{W_{st}}{A_r} - \frac{W_e}{A_r} - \frac{W_r}{A_r} - \frac{W_{sh}}{A_r} \tag{B26}$$

The airplane structure weight was assumed to be equal to 40 percent of the gross weight. The ratio of disposable load to gross weight is then

$$\frac{W_d}{W_g} = 0.6 - \frac{\frac{W_e}{M}\frac{M}{A_r} + \rho_r l(1-f) + \frac{W_{sh}}{A_r}}{\left(\frac{F}{A_r} - \frac{D_n}{A_r}\right)\frac{L}{D}} \tag{B27}$$

APPENDIX C

EQUATIONS FOR TOTAL-TEMPERATURE AND TOTAL-PRESSURE RATIO ACROSS REACTOR

Temperature Ratio across Reactor

In the development of the charts of reference 3, which give the pressure drop in a tube for the case of heat being added at a constant tube-wall temperature, the pressure drop is shown to be a function of an effective length-to-diameter ratio of the tubes, which is defined by equation (C8) in this appendix. It is shown here that the ratio of the total temperature at the reactor outlet to the total temperature at the reactor inlet is a function of this same effective length-to-diameter ratio for a specified tube-wall and reactor-inlet temperature. For most of the calculations, the turbine-inlet temperature T_7 was specified and used to calculate a value of $(l/d)_{eff}$ that is then used to compute the reactor pressure drop.

It was assumed that there was no change in total temperature from station 4 to station 5 or from station 6 to station 7 so that

$$\frac{T_5}{T_6} = \frac{T_4}{T_7} \tag{C1}$$

The heat transferred from the tube to the air in the incremental length dx is

$$dQ = Mgc_{p,b}\, dT = hs(T_w - T)\, dx \tag{C2}$$

or

$$\frac{dT}{T_w - T} = \frac{hs}{Mgc_{p,b}}\, dx \tag{C3}$$

where T is the total temperature of the air in the tube. Integrating equation (C3) from the tube inlet (station 5) to the tube outlet (station 6) for a constant tube-wall temperature with the assumtion of constant average values for the heat-transfer coefficient and specific heat gives

$$-\log_e \frac{T_w - T_6}{T_w - T_5} = \frac{hsl}{Mgc_{p,b}} \tag{C4}$$

Substituting the total tube surface area S for sl, T_4 for T_5, and T_7 for T_6 and rearranging give

$$\frac{T_7}{T_4} = 1 + \left(\frac{T_w}{T_4} - 1\right)\left(1 - e^{-hS/(Mgc_{p,b})}\right) \tag{C5}$$

The modified Nusselt equation for heat transfer at high tube-wall temperatures, as given in reference 5, is

$$\frac{hd}{k_w} = 0.023 \left(\frac{\rho_w v d}{\mu_w}\right)^{0.8} \left(\frac{c_{p,w}\mu_w}{k_w}\right)^{0.4} \tag{C6}$$

With the use of the continuity equation, the relation between the tube flow area and tube surface area, and the value of h from equation (C6), the exponent of e in equation (C5) becomes

$$\frac{hS}{Mgc_{p,b}} = 0.092 \frac{19.22}{19.22} \left(\frac{k_w}{c_{p,w}\mu_w}\right)^{0.6} \left(\frac{\rho_b v d}{\mu_w}\right)^{-0.2} \left(\frac{\rho_w}{\rho_b}\right)^{0.8} \frac{c_{p,w}}{c_{p,b}} \frac{l}{d} \tag{C7}$$

For convenience, let

$$\left(\frac{l}{d}\right)_{eff} = 19.22 \left(\frac{M}{A_r} \frac{gd}{f\mu_w}\right)^{-0.2} \left(\frac{\rho_w}{\rho_b}\right)^{0.8} \frac{c_{p,w}}{c_{p,b}} \frac{l}{d} \tag{C8}$$

where

$$\frac{M}{A_r} \frac{g}{f} = \frac{\dot{M}}{A_f} g = \rho_b v \tag{C9}$$

An average value for the Prandtl number evaluated at the tube-wall temperature of 0.752 was assumed. Combining equations (C7) and (C8) and substituting this value of Prandtl number give

$$\frac{hS}{Mgc_{p,b}} = 0.00568\left(l/d\right)_{eff} \tag{C10}$$

From equations (C5) and (C10),

$$\frac{T_7}{T_4} = 1 + \left(\frac{T_w}{T_4} - 1\right)\left(1 - e^{-0.00568(l/d)_{eff}}\right) \tag{C11}$$

The total-temperature ratio across the reactor T_7/T_4 is thus a function of the tube-wall temperature, the air temperature at the reactor inlet, and the effective reactor passage length-to-diameter ratio as defined by equation (C8).

Pressure Ratio across Reactor

An accurate determination of the pressure changes of a compressible fluid flowing through heat-exchanger passages at high flow Mach numbers and high rates of heating requires a numerical integration for each specific set of conditions. In reference 3 charts are presented that enable the determination, without individual integration, of the pressure drop of a compressible fluid flowing through heat-exchanger passages. These charts account for the effect on the heat-exchanger flow process of high temperature differentials between the passage wall and the fluid, which was experimentally investigated in reference 5. The charts are set up for heat transfer from a passage wall at constant temperature throughout its length to air (constant ratio of specific heats) flowing in turbulent motion and yield a solution for the pressure drop when the tube-wall temperature, the mass flow of air per unit flow area, the effective length-to-diameter ratio (see equation (C8)), and the total temperature and pressure at the tube inlet are specified. That portion of the reactor pressure drop from station 5 to station 6 was determined from these charts.

The variation of the pressure ratio across the reactor P_5/P_6 with mass flow per unit reactor frontal area M/A_r is shown in

figure 16 for various compressor pressure ratios P_4/P_1 as calculated from the charts of reference 3. Figures 16(a) to 16(e) are for the five different combinations of altitude, tube-wall temperature, turbine-inlet temperature, and reactor free-flow-area ratio for which performance calculations were made.

For a constant compressor pressure ratio, increasing the mass flow per unit reactor frontal area increases the total-pressure ratio (that is, the total-pressure drop) across the reactor. Inasmuch as the free-flow-area ratio is constant, an increase in mass flow per unit frontal area is equivalent to an increase in mass flow per unit flow area or tube area. The slope of these curves approaches infinity as the mass flow is increased, indicating that the choke condition or the critical pressure ratio is being approached at the upper end of the curves. For a constant mass flow per unit reactor frontal area, decreasing the compressor pressure ratio increases the total pressure ratio across the reactor; or, for a constant pressure ratio across the reactor, increasing the compressor pressure ratio allows an increase in the mass flow of air per unit reactor frontal area.

Although no specific plan for passing the air in and out of the end shielding is recommended herein, pressure drops for these portions of the system of approximately $\frac{1}{2}\rho v^2$ were assumed as follows:

$$\Delta P_{4-5} = \frac{g}{2}\left(\frac{M}{A_r}\right)^2 \frac{RT_4}{P_4} \qquad (C12)$$

and

$$\Delta P_{6-7} = \frac{g}{2}\left(\frac{M}{A_r}\right)^2 \frac{RT_6}{P_6} \qquad (C13)$$

APPENDIX D

ENGINE FRONTAL AREA AND WEIGHT

The air flow per unit of engine (compressor) frontal area was assumed to be 25 pounds per second per square foot at sea-level static conditions, which is approximately the highest air handling capacity of current turbojet engines. This air flow per unit compressor frontal area was then varied with compressor-inlet temperature and pressure T_1 and P_1 as follows:

$$\frac{W}{A_e} = \left(\frac{W}{A_e}\right)_s \frac{P_1}{\sqrt{T_1}} \frac{\sqrt{519}}{2116.4} \tag{D1}$$

Substituting a base air flow per unit frontal area $(W/A_e)_s$ of 25 pounds per second per square foot gives, from equation (D1),

$$\frac{W}{A_e} = \frac{0.269\ P_1}{\sqrt{T_1}} \tag{D2}$$

The engine weights were calculated according to a method that assumes the engine weight to be a function of the compressor pressure ratio, altitude, and flight speed. The basic components of the turbojet engine for which weights were separately calculated are the compressor, the turbine, and the shafting. The compressor for this analysis is considered to be of the axial-flow type and is divided into two parts: the rotor consisting of the sum of the compressor disks with their rims and blades, and the shell with its stators. The turbine rotor and shell are also separately calculated. The compressor is considered to be designed on the basis of a constant axial Mach number and a constant Reynold's number throughout the compressor. The specific engine weights (lb of engine / lb of working air/sec), as calculated herein, are independent of the engine size.

The weight of the intercooler was estimated using the charts of reference 6. A ratio of cooling-air pressure drop to compressible dynamic pressure of 0.20, an engine-air pressure drop of 1 inch of mercury, a ratio of cooling air to engine air of 2.0, and a cooling effectiveness of 0.50 were assumed. Average values were used for the cooling-air side and engine-air side pressures, temperatures, and temperature rises. The effect of the engine-air

side pressure drop on the thrust of the system was neglected and the intercooler was assumed to have little or no internal drag power. The intercooler weight, as estimated from reference 6 including a 40-percent increase to allow for spacers, headers, and other structural parts, was 10 pounds per pound per second of air flow.

The following table lists the engine weights (including the intercooler weight) per pound per second of air used in this analysis:

Altitude	Compressor pressure ratio	Engine weight per unit air flow (lb/(lb/sec))
30,000	10	45
	20	59
	30	70
	40	81
	50	92
50,000	10	88
	20	120
	30	146
	40	167
	50	188

The reactor, which constituted only a small portion (1 to 10 percent) of the total system weight, was assumed to have a specific gravity of 2.0.

REFERENCES

1. Humble, Leroy V., and Doyle, Ronald B.: Calculated Condenser Performance for a Steam-Turbine Power Plant for Aircraft. NACA RM E7J01, 1947.

2. Pinkel, Benjamin, and Karp, Irving M.: A Thermodynamic Study of the Turbojet Engine. NACA Rep. 891, 1947.

3. Valerino, Michael F.: Generalized Charts for Determination of Pressure Drop of a High-Speed Compressible Fluid in Heat-Exchanger Passages. I - Air Heated in Smooth Passages of Constant Area with Constant Wall Temperature. NACA RM E8G23, 1948.

4. Diehl, Walter S.: Standard Atmosphere - Tables and Data. NACA Rep. 218, 1925.

5. Lowdermilk, Warren H., and Grele, Milton D.: Heat Transfer from High-Temperature Surfaces to Fluids. II - Correlation of Heat-Transfer and Friction Data for Air Flowing in Inconel Tube with Rounded Entrance. NACA RM E8L03, 1949.

6. Pinkel, Benjamin, Reuter, J. George, and Valerino, Michael F.: The Cross-Flow Plate-Type Intercooler. NACA ACR, April 1942.

Station

0 Ambient conditions
1 Compressor inlet
2 Intercooler inlet
3 Intercooler outlet
4 Compressor outlet
5 Reactor-tube inlet
6 Reactor-tube outlet
7 Turbine inlet

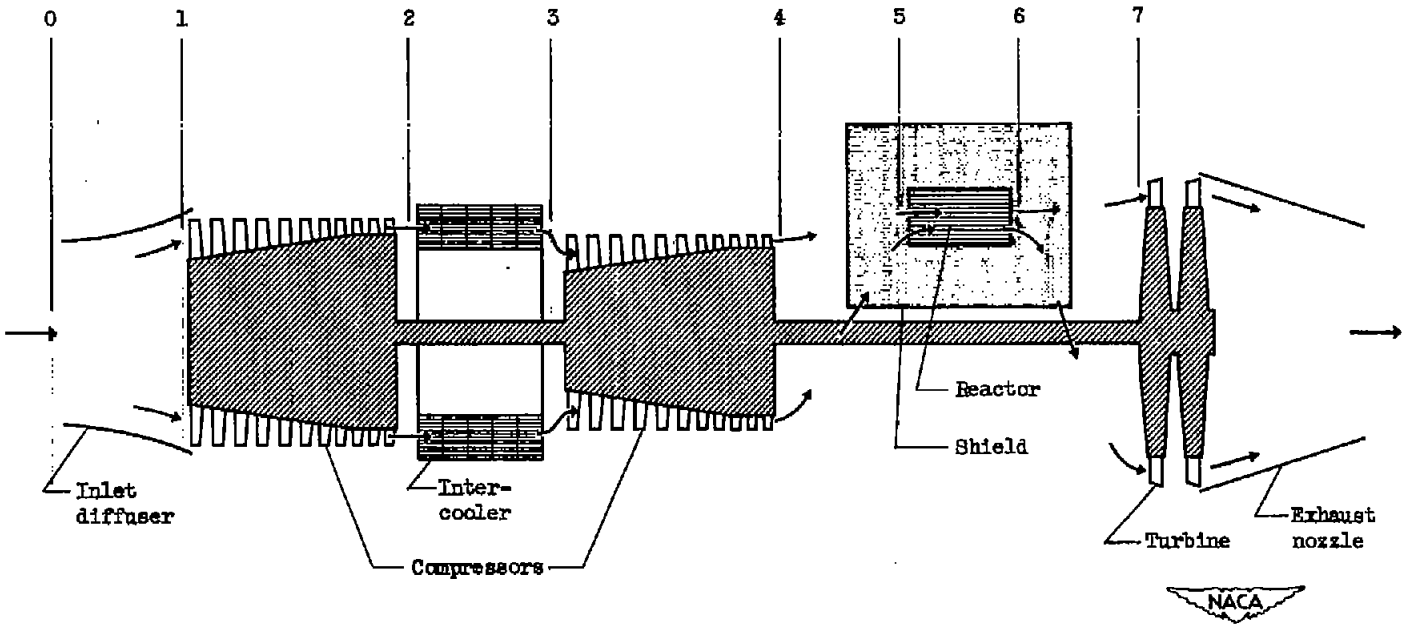

Figure 1. - Schematic diagram of turbojet engine.

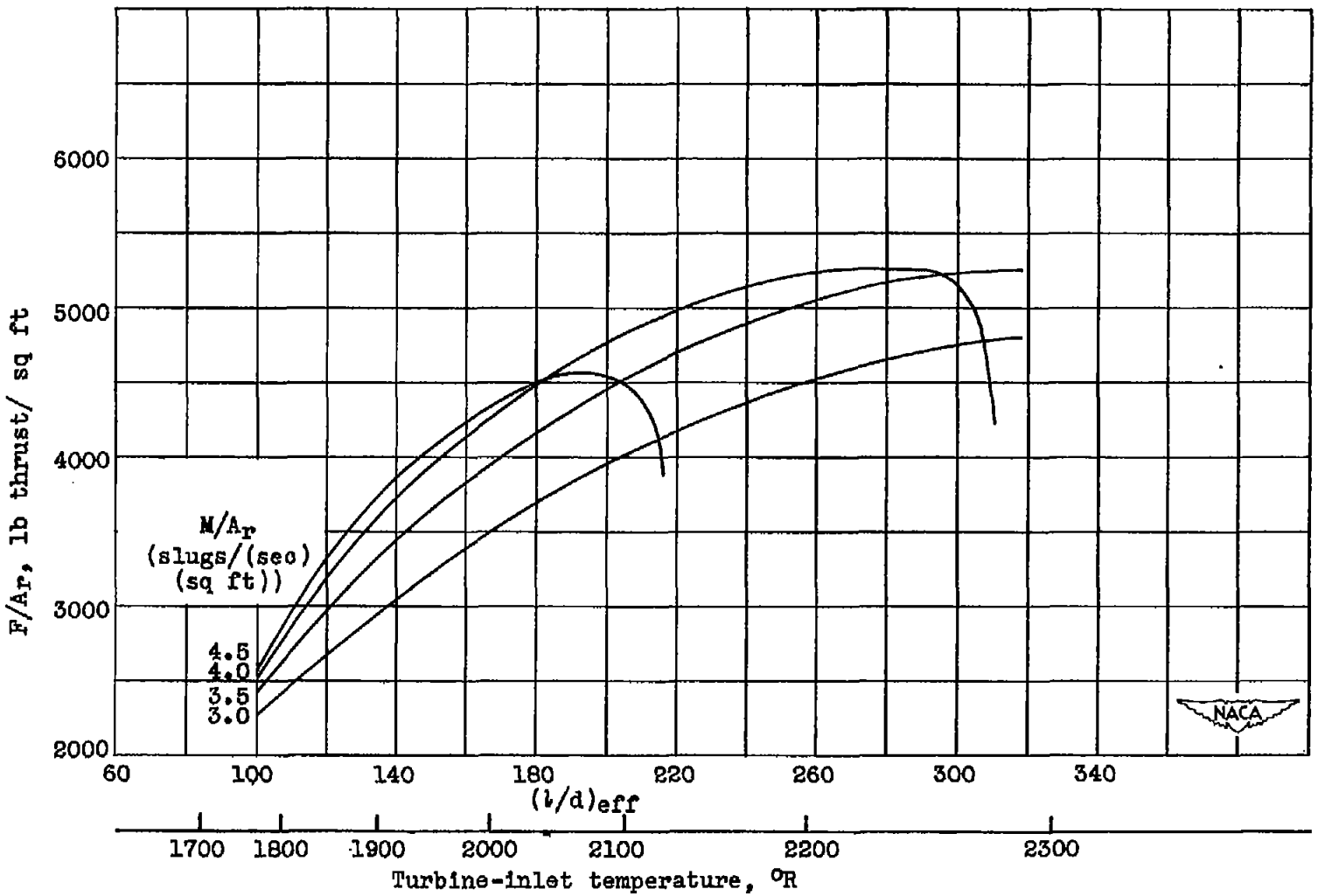

Figure 2. - Variation of thrust per unit reactor frontal area F/A_r with effective length-to-diameter ratio $(l/d)_{eff}$ for various mass flows per unit reactor frontal area M/A_r. Flight Mach number, 0.9; altitude, 30,000 feet; tube-wall temperature, 2500° R; compressor pressure ratio, 40; reactor free-flow-area ratio, 0.50.

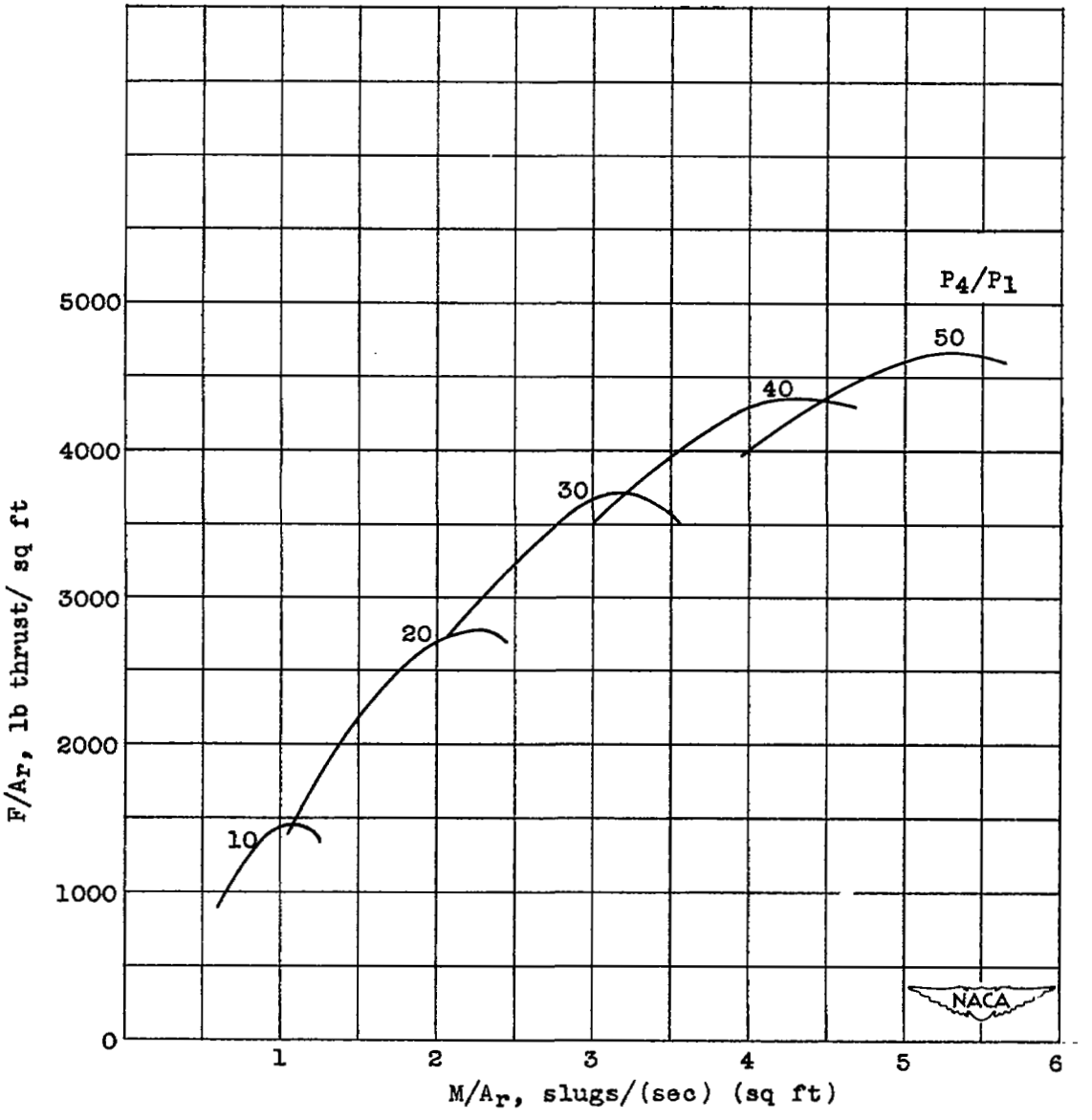

Figure 3. - Variation of thrust per unit reactor frontal area F/A_r with mass flow per unit reactor frontal area M/A_r for various compressor pressure ratios P_4/P_1. Flight Mach number, 0.9; altitude, 30,000 feet; tube-wall temperature, 2500° R; turbine-inlet temperature, 2000° R; reactor free-flow-area ratio, 0.50.

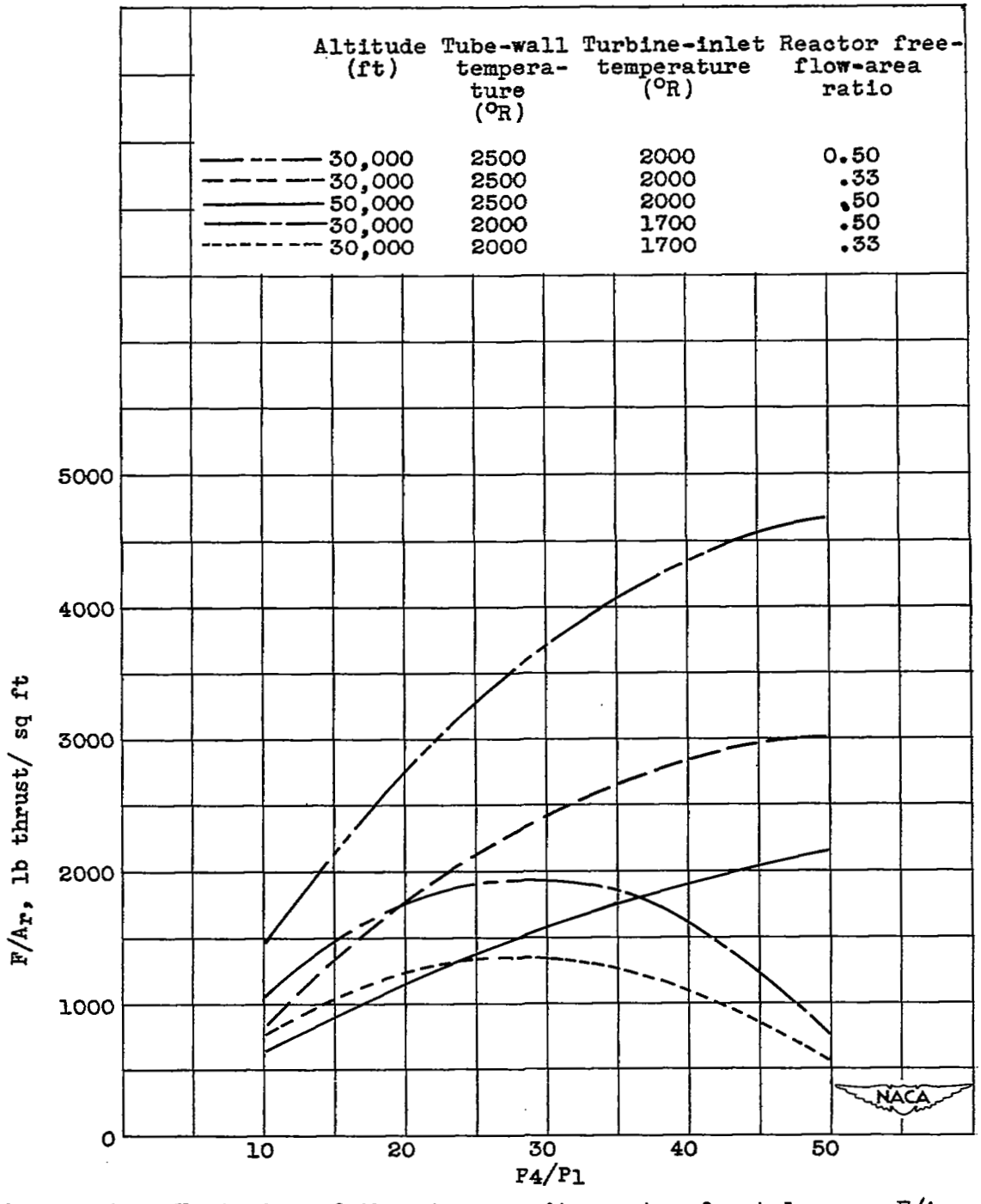

Figure 4. - Variation of thrust per unit reactor frontal area F/Ar with compressor pressure ratio P_4/P_1. Mass flow per unit reactor frontal area for maximum thrust per unit reactor frontal area; flight Mach number, 0.9.

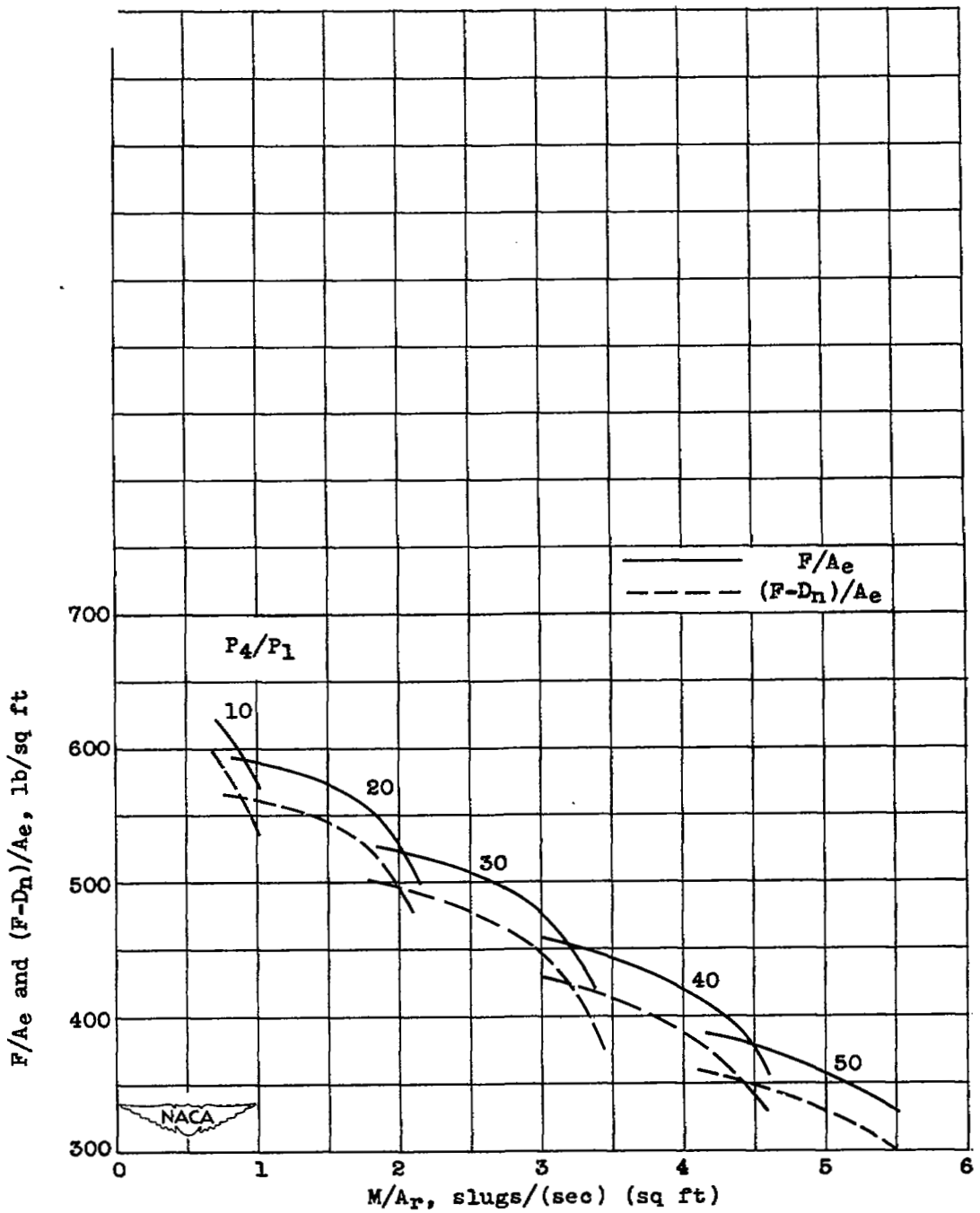

Figure 5. - Variation of thrust and net thrust per unit engine frontal area F/A_e and $(F-D_n)/A_e$ with mass flow per unit reactor frontal area M/A_r for various compressor pressure ratios P_4/P_1. Flight Mach number, 0.9; altitude, 30,000 feet; tube-wall temperature, 2500° R; turbine-inlet temperature, 2000° R; reactor free-flow-area ratio, 0.50.

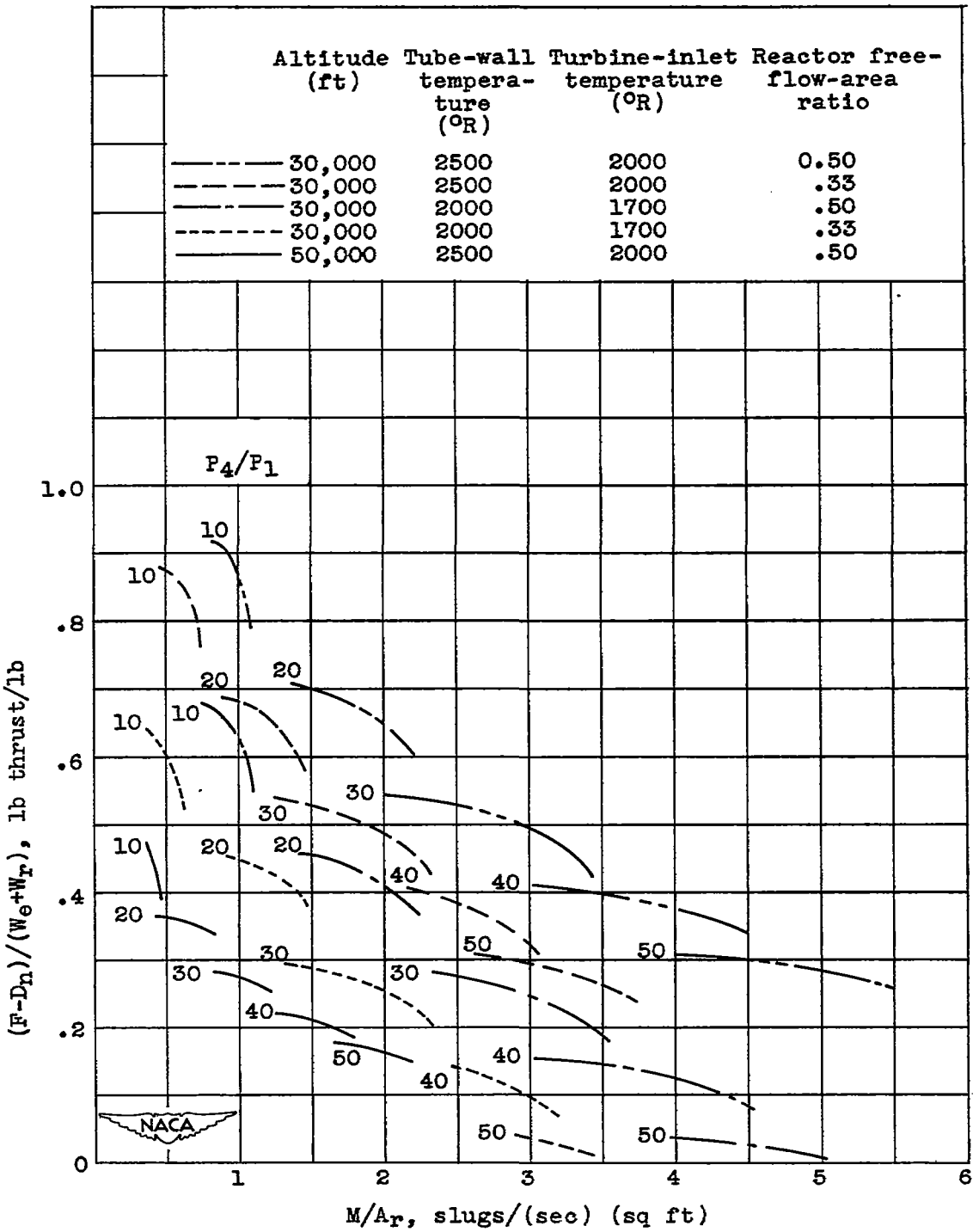

Figure 6. - Variation of net thrust per unit engine weight plus reactor weight $(F-D_n)/(W_e+W_r)$ with mass flow per unit reactor frontal area M/A_r for various compressor pressure ratios P_4/P_1. Flight Mach number, 0.9; reactor length, 2 feet.

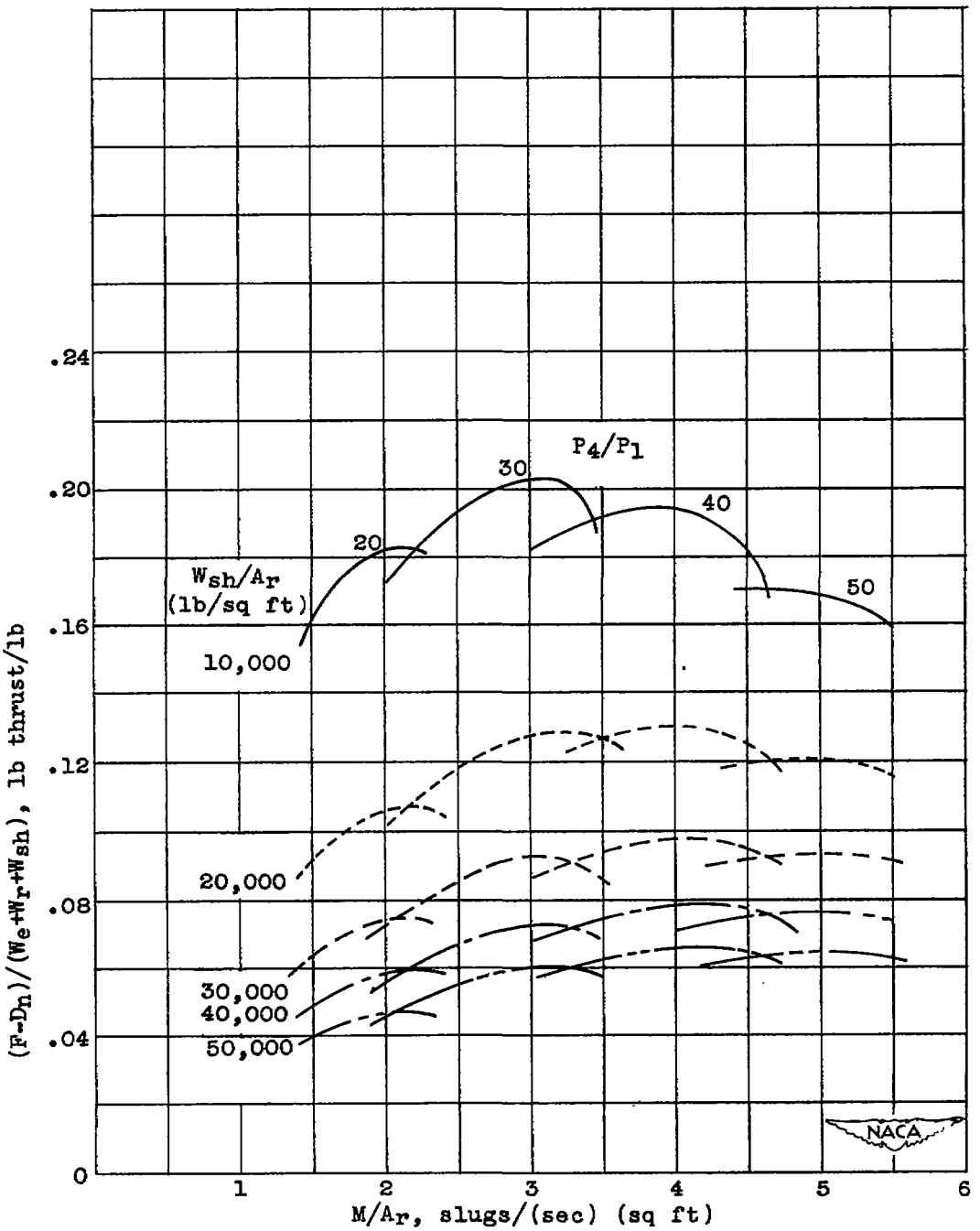

Figure 7. - Variation of net thrust per unit of engine plus reactor plus shielding weight $(F-D_n)/(W_e+W_r+W_{sh})$ with mass flow per unit reactor frontal area M/A_r for various compressor pressure ratios P_4/P_1 and shielding weights per unit reactor frontal area W_{sh}/A_r. Flight Mach number, 0.9; altitude, 30,000 feet; tube-wall temperature, 2500° R; turbine-inlet temperature, 2000° R; reactor free-flow-area ratio, 0.50; reactor length, 2 feet.

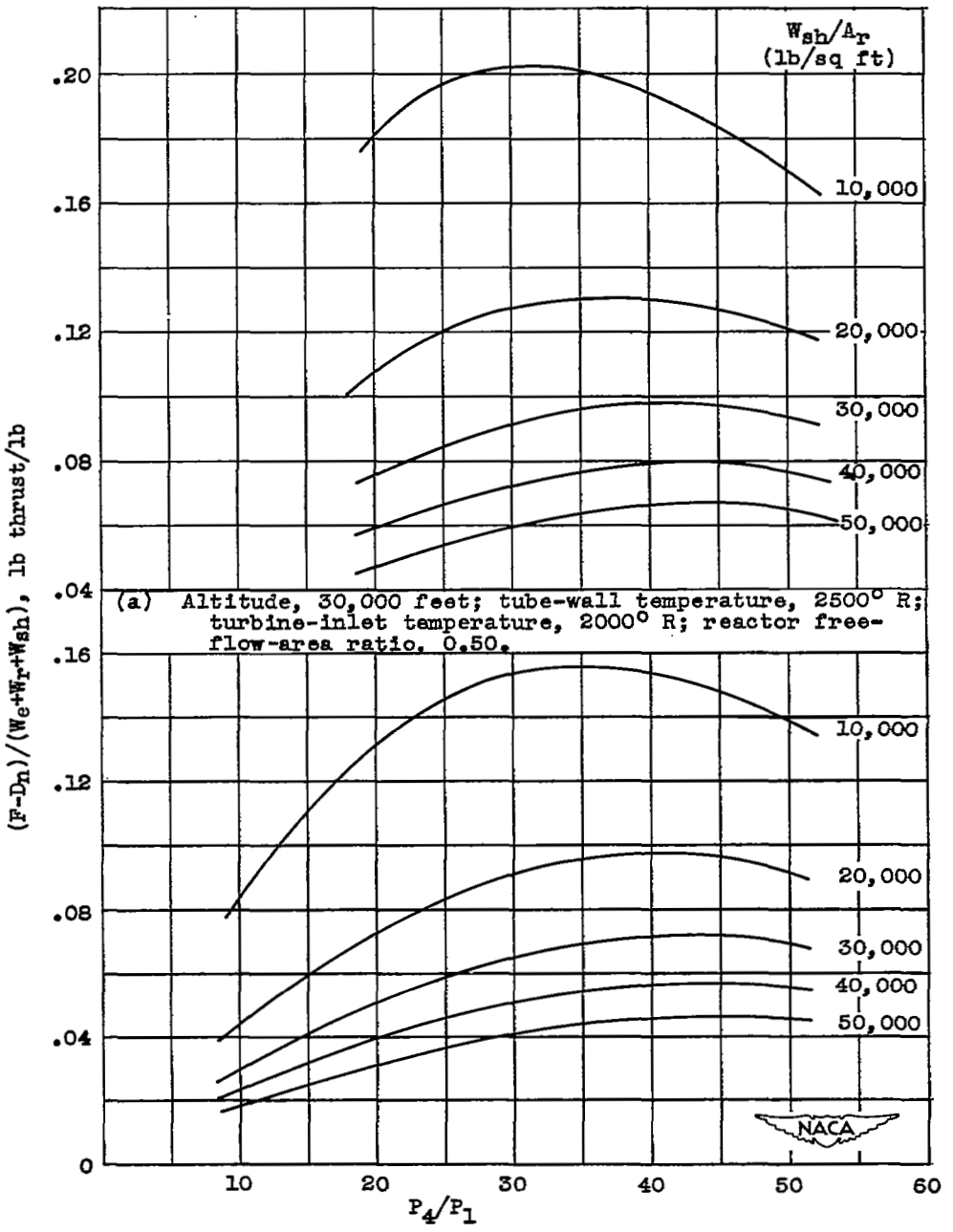

(a) Altitude, 30,000 feet; tube-wall temperature, 2500° R; turbine-inlet temperature, 2000° R; reactor free-flow-area ratio, 0.50.

(b) Altitude, 30,000 feet; tube-wall temperature, 2500° R; turbine-inlet temperature, 2000° R; reactor free-flow-area ratio, 0.33.

Figure 8. - Variation of net thrust per unit of engine plus reactor plus shielding weight $(F-D_n)/(W_e+W_r+W_{sh})$ with compressor pressure ratio P_4/P_1 for various shielding weights per unit reactor frontal area W_{sh}/A_r. Mass flow per unit reactor frontal area for maximum specific weight; flight Mach number, 0.9; reactor length, 2 feet.

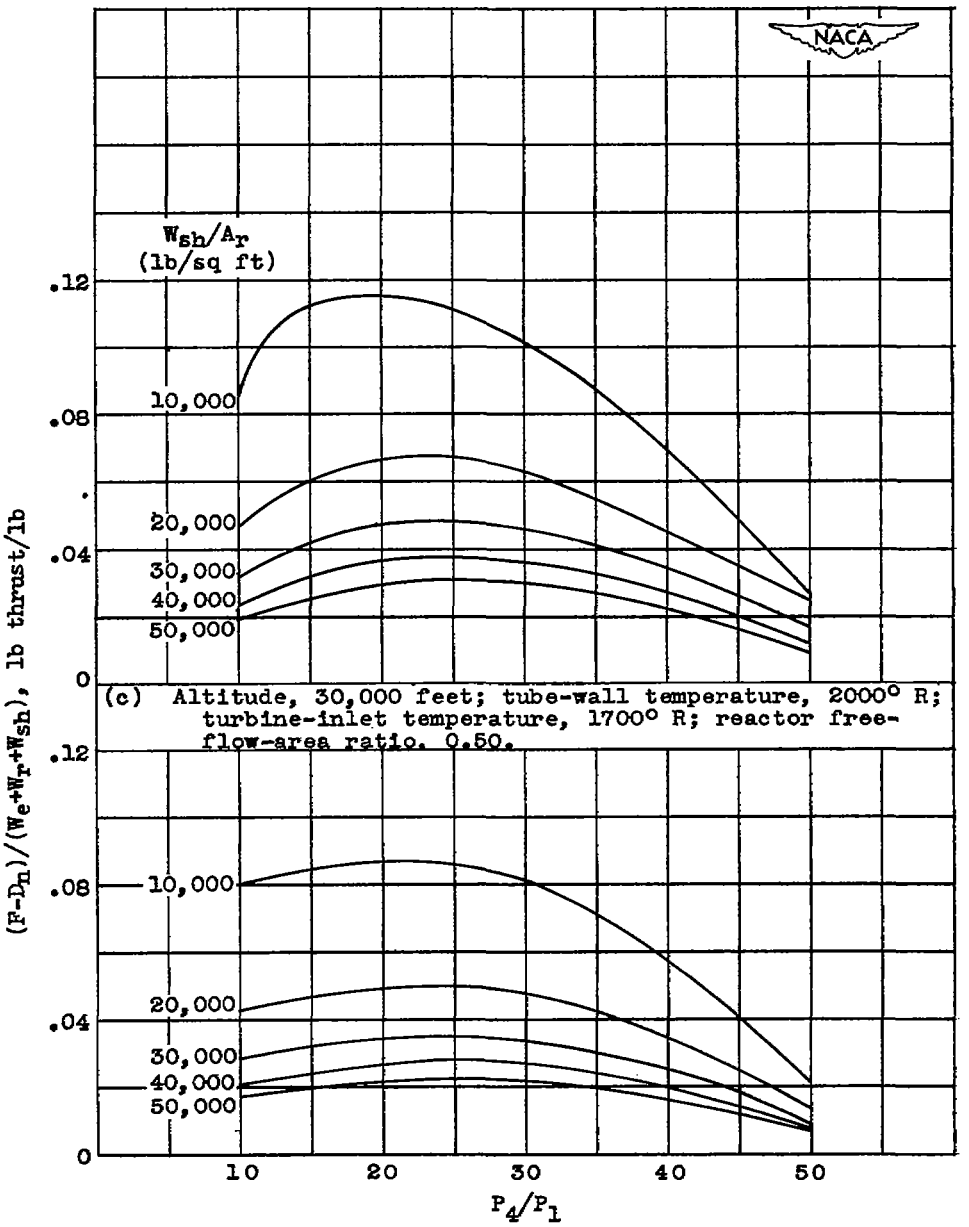

(c) Altitude, 30,000 feet; tube-wall temperature, 2000° R; turbine-inlet temperature, 1700° R; reactor free-flow-area ratio, 0.50.

(d) Altitude, 30,000 feet; tube-wall temperature, 2000° R; turbine-inlet temperature, 1700° R; reactor free-flow-area ratio, 0.33.

Figure 8. - Continued. Variation of net thrust per unit of engine plus reactor plus shielding weight $(F-D_n)/(W_e+W_r+W_{sh})$ with compressor pressure ratio P_4/P_1 for various shielding weights per unit reactor frontal area W_{sh}/A_r. Mass flow per unit reactor frontal area for maximum specific weight; flight Mach number, 0.9; reactor length, 2 feet.

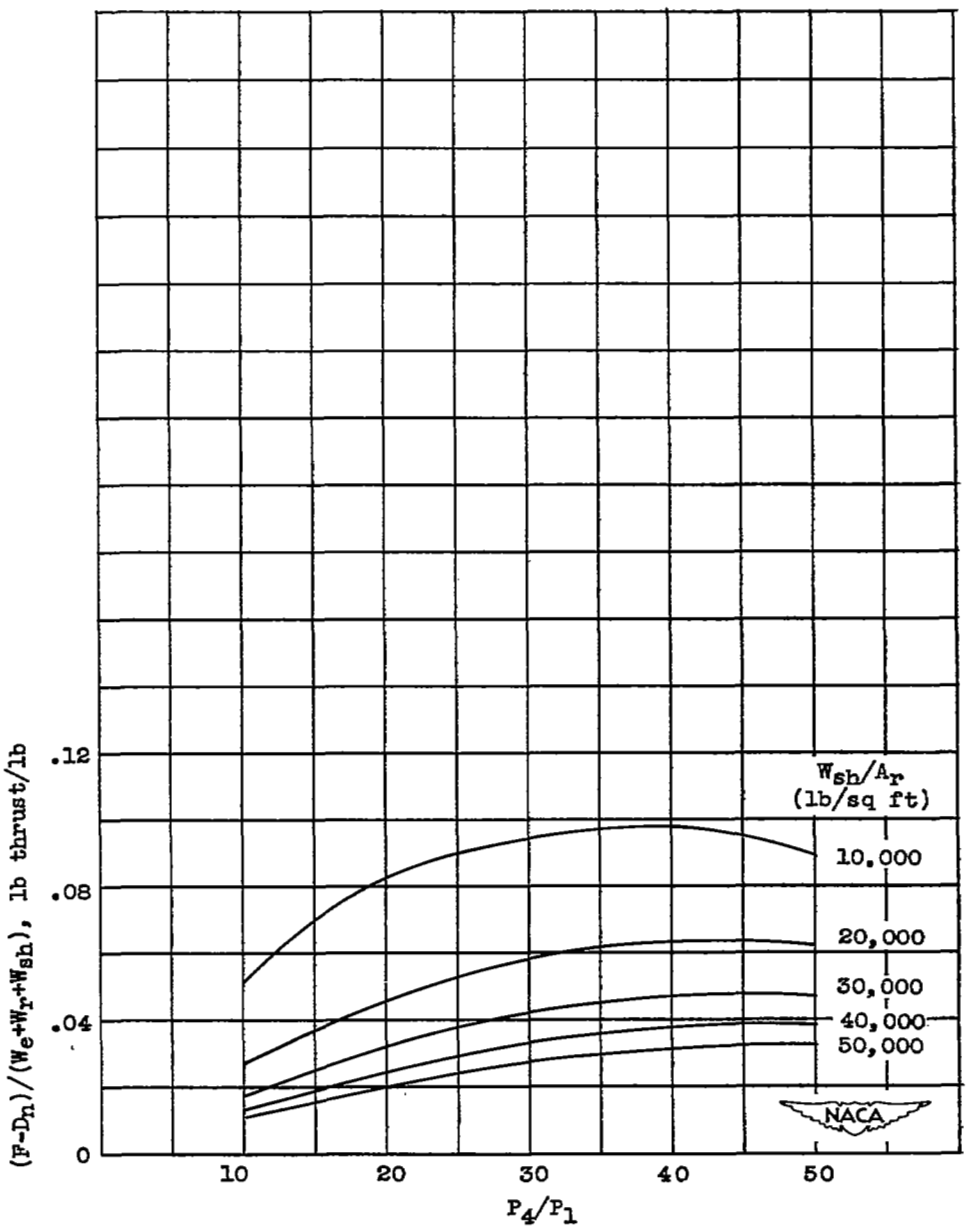

(e) Altitude, 50,000 feet; tube-wall temperature, 2500° R; turbine-inlet temperature, 2000° R; reactor free-flow-area ratio, 0.50.

Figure 8. - Concluded. Variation of net thrust per unit of engine plus reactor plus shielding weight $(F-D_n)/(W_e+W_r+W_{sh})$ with compressor pressure ratio P_4/P_1 for various shielding weights per unit reactor frontal area W_{sh}/A_r. Mass flow per unit reactor frontal area for maximum specific weight; flight Mach number, 0.9; reactor length, 2 feet.

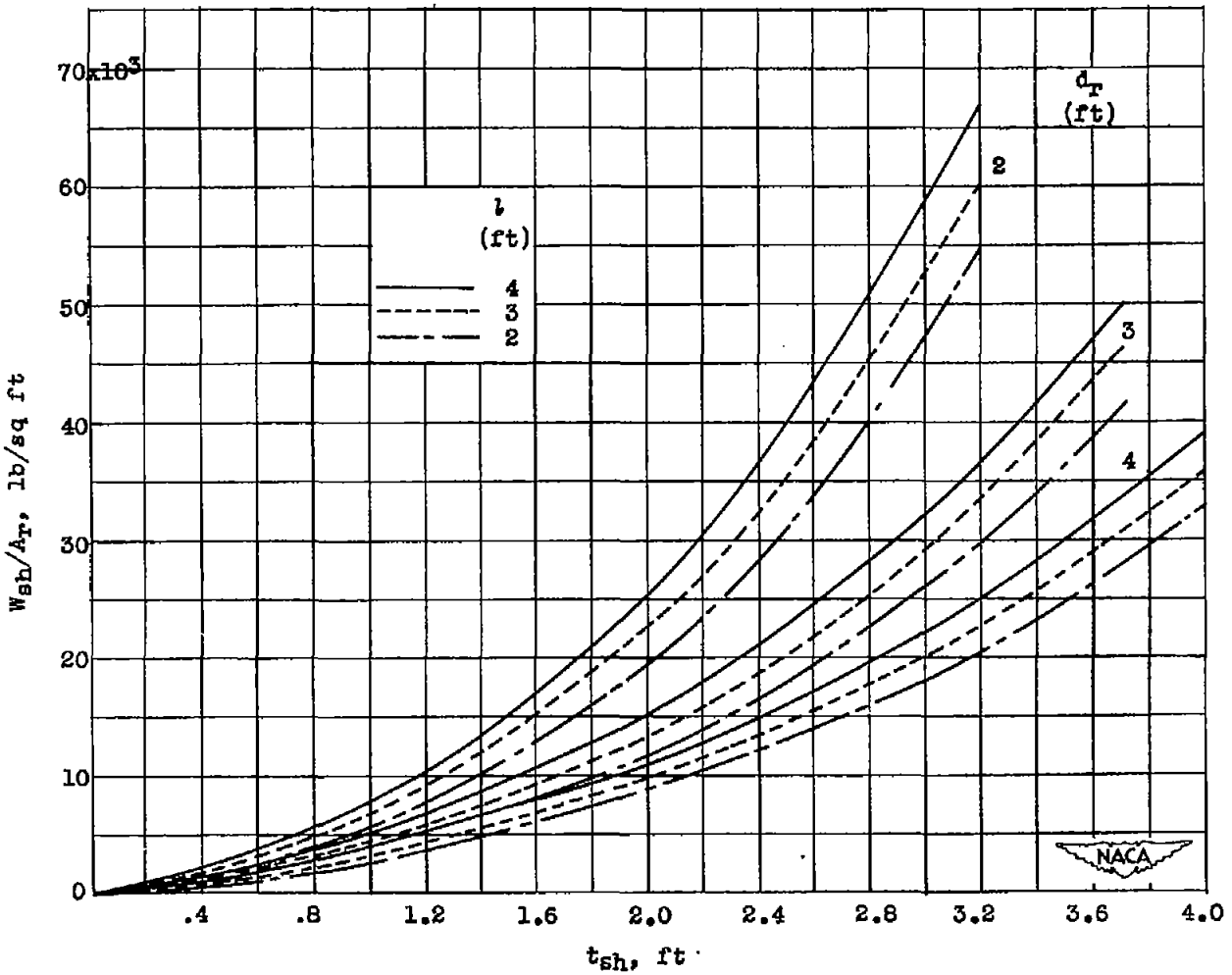

Figure 9. - Variation of shielded reactor weight per unit reactor frontal area W_{sh}/A_r with shielding thickness t_{sh}, reactor diameter d_r, and reactor length l. Specific gravity of shielding material, 6.0.

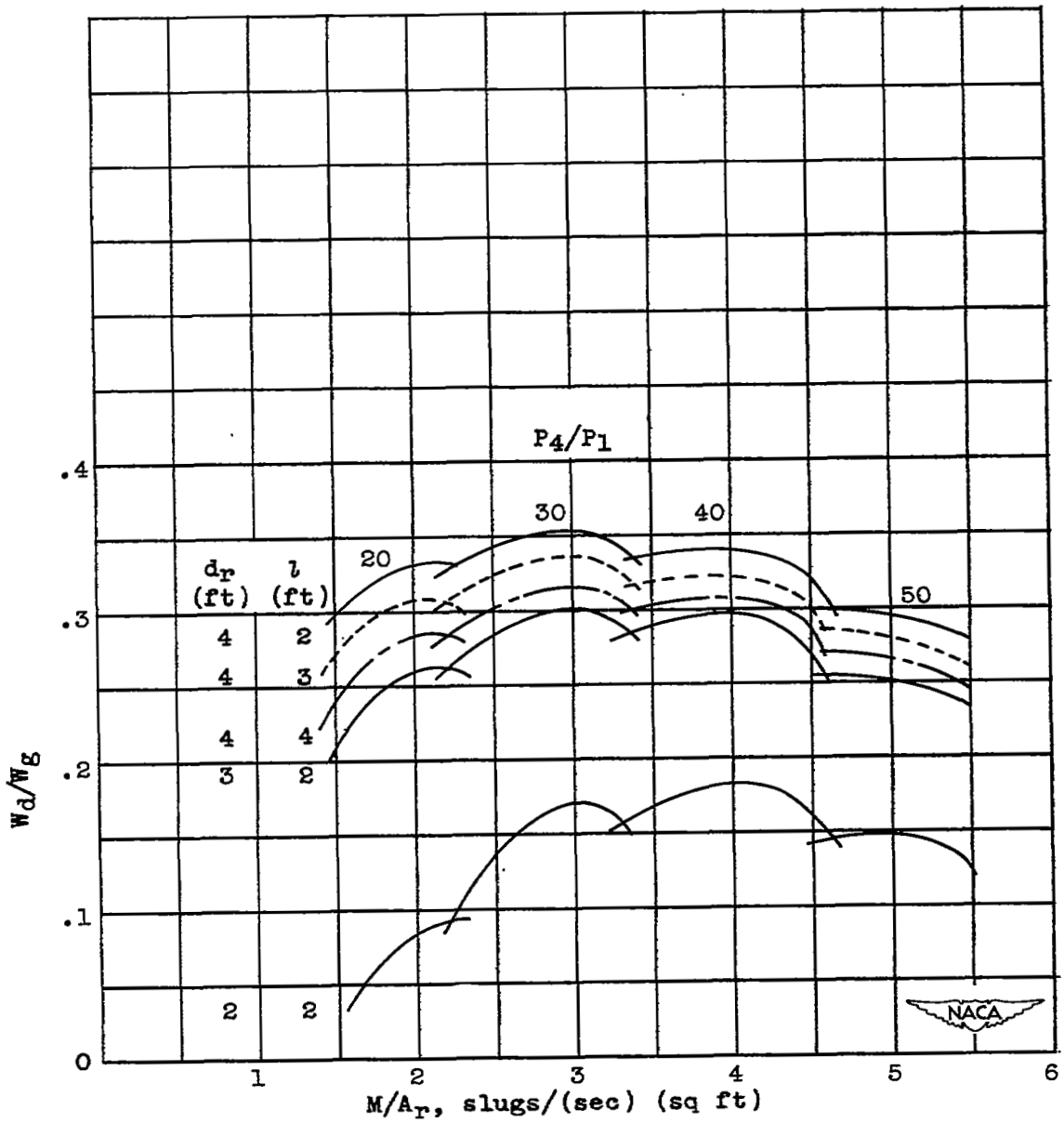

Figure 10. - Variation of ratio of disposable load to airplane gross weight W_d/W_g with mass flow per unit reactor frontal area M/A_r for various compressor pressure ratios P_4/P_1, reactor diameters d_r, and reactor lengths l. Flight Mach number, 0.9; altitude, 30,000 feet; tube-wall temperature, 2500° R; turbine-inlet temperature, 2000° R; reactor free-flow-area ratio, 0.50; shielding thickness, 2 feet; specific gravity of shielding, 6.0; lift-drag ratio, 18; airplane structural weight, 0.4 airplane gross weight.

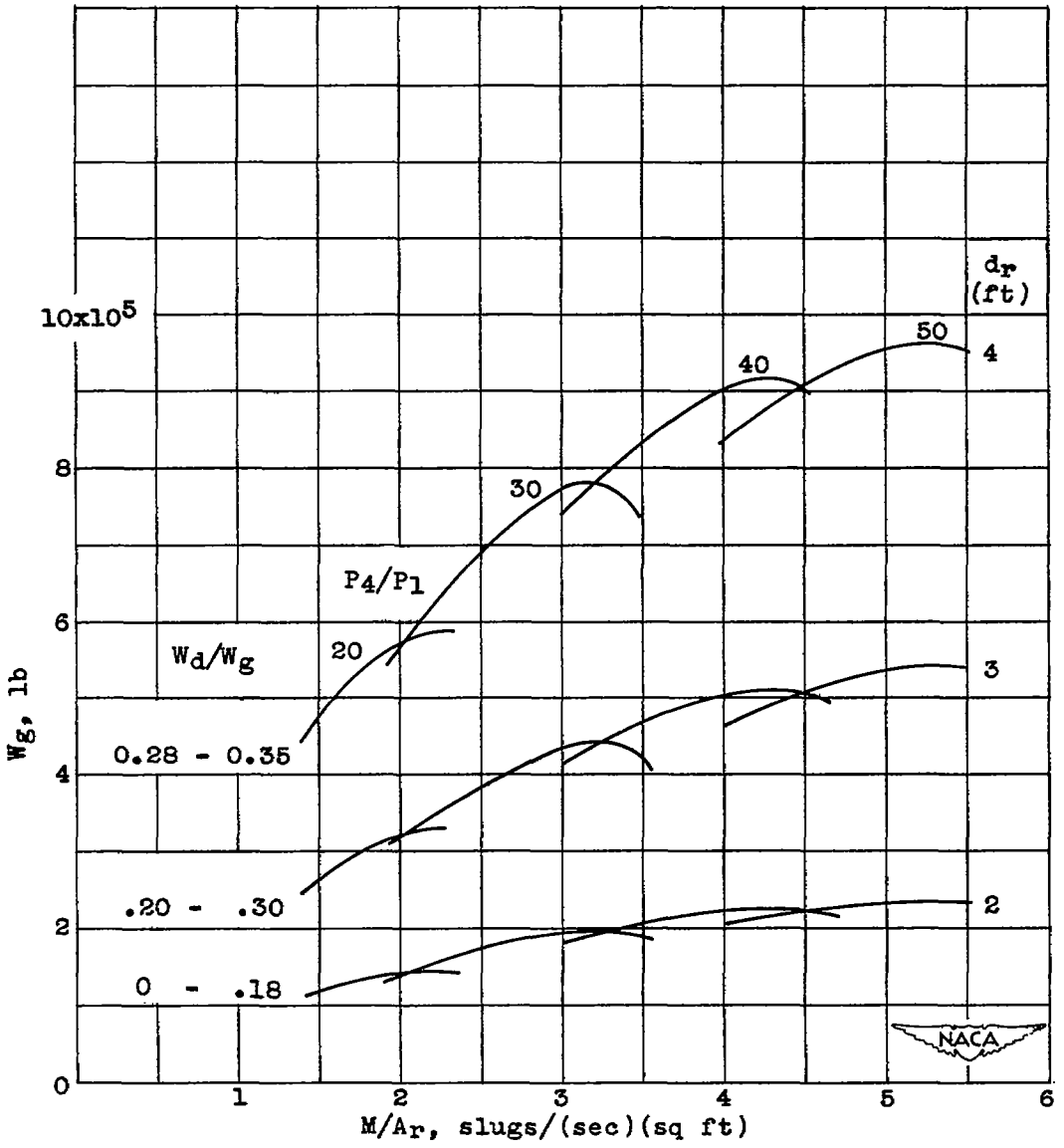

Figure 11. - Variation of airplane gross weight W_g with mass flow per unit reactor frontal area M/A_r for various compressor pressure ratios P_4/P_1 and reactor diameters d_r. Flight Mach number, 0.9; altitude, 30,000 feet; tube-wall temperature, 2500° R; turbine-inlet temperature, 2000° R; reactor free-flow-area ratio, 0.50; reactor length, 2 feet; shielding thickness, 2 feet; specific gravity of shielding, 6.0; lift-drag ratio, 18; airplane structural weight, 0.4 airplane gross weight.

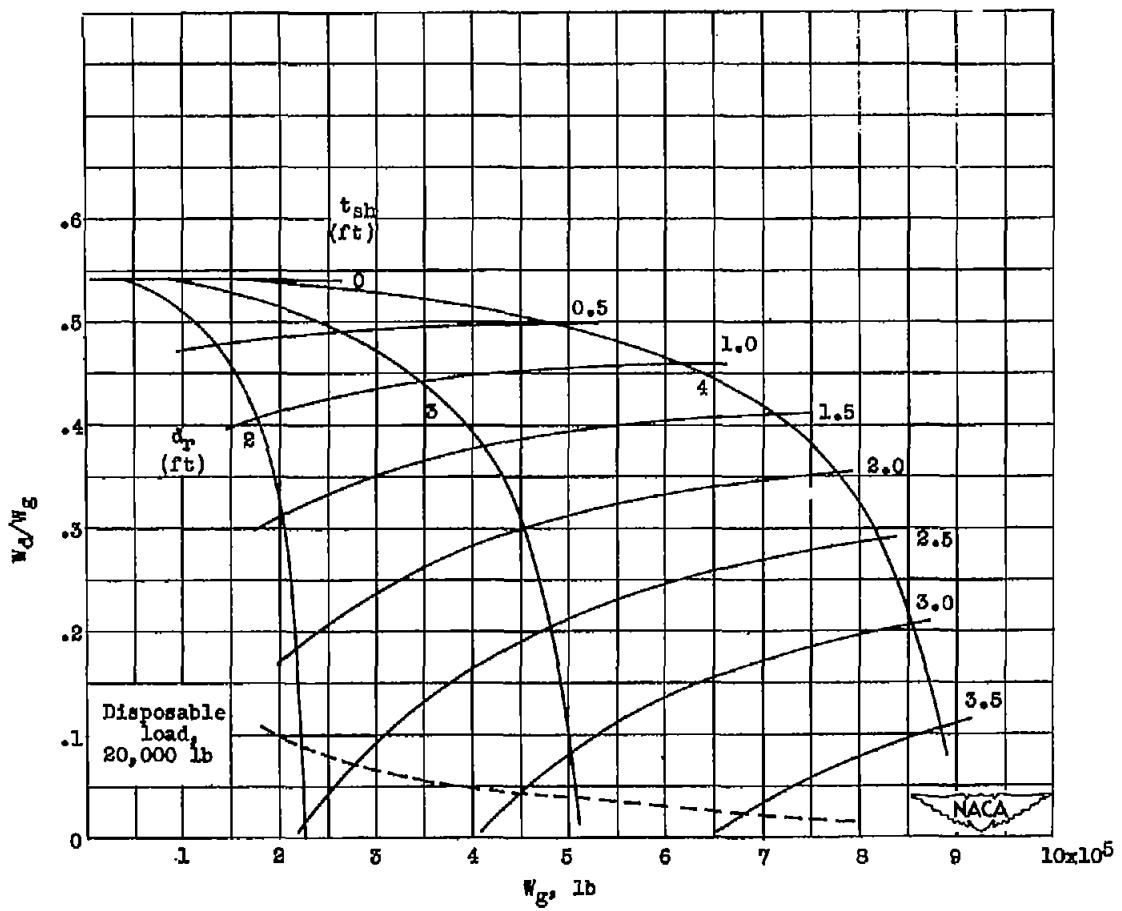

(a) Altitude, 30,000 feet; tube-wall temperature, 2500° R; turbine-inlet temperature, 2000° R; reactor free-flow-area ratio, 0.50.

Figure 12. - Variation of ratio of disposable load to airplane gross weight W_d/W_g with airplane gross weight W_g for various reactor diameters d_r and shielding thicknesses t_{sh}. Mass flow per unit reactor frontal area and compressor pressure ratio for maximum ratio of disposable load to airplane gross weight; flight Mach number, 0.9; reactor length, 2 feet; specific gravity of shielding, 6.0; lift-drag ratio, 18; airplane structural weight, 0.4 airplane gross weight.

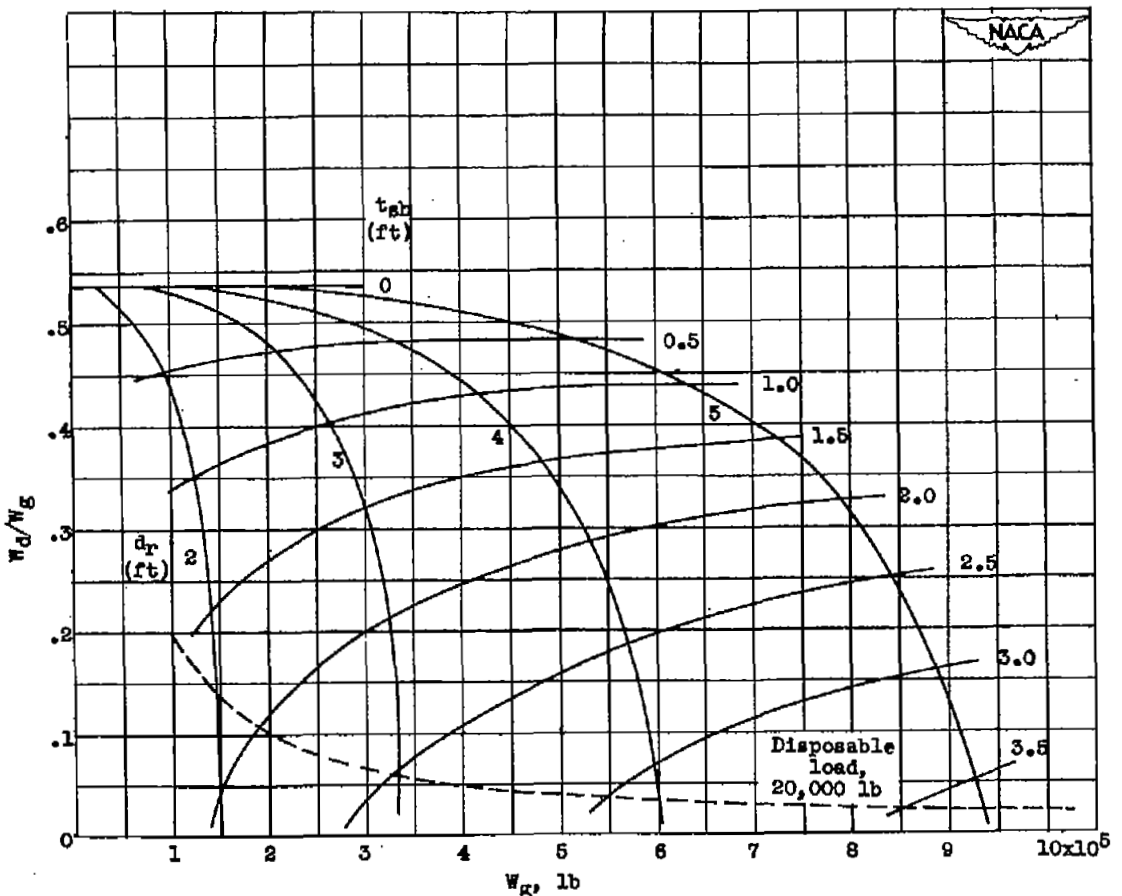

(b) Altitude, 30,000 feet; tube-wall temperature, 2500° R; turbine-inlet temperature, 2000° R; reactor free-flow-area ratio, 0.33.

Figure 12. - Continued. Variation of ratio of disposable load to airplane gross weight W_d/W_g with airplane gross weight W_g for various reactor diameters d_r and shielding thicknesses t_{sh}. Mass flow per unit reactor frontal area and compressor pressure ratio for maximum ratio of disposable load to airplane gross weight; flight Mach number, 0.9; reactor length, 2 feet; specific gravity of shielding, 6.0; lift-drag ratio, 18; airplane structural weight, 0.4 airplane gross weight.

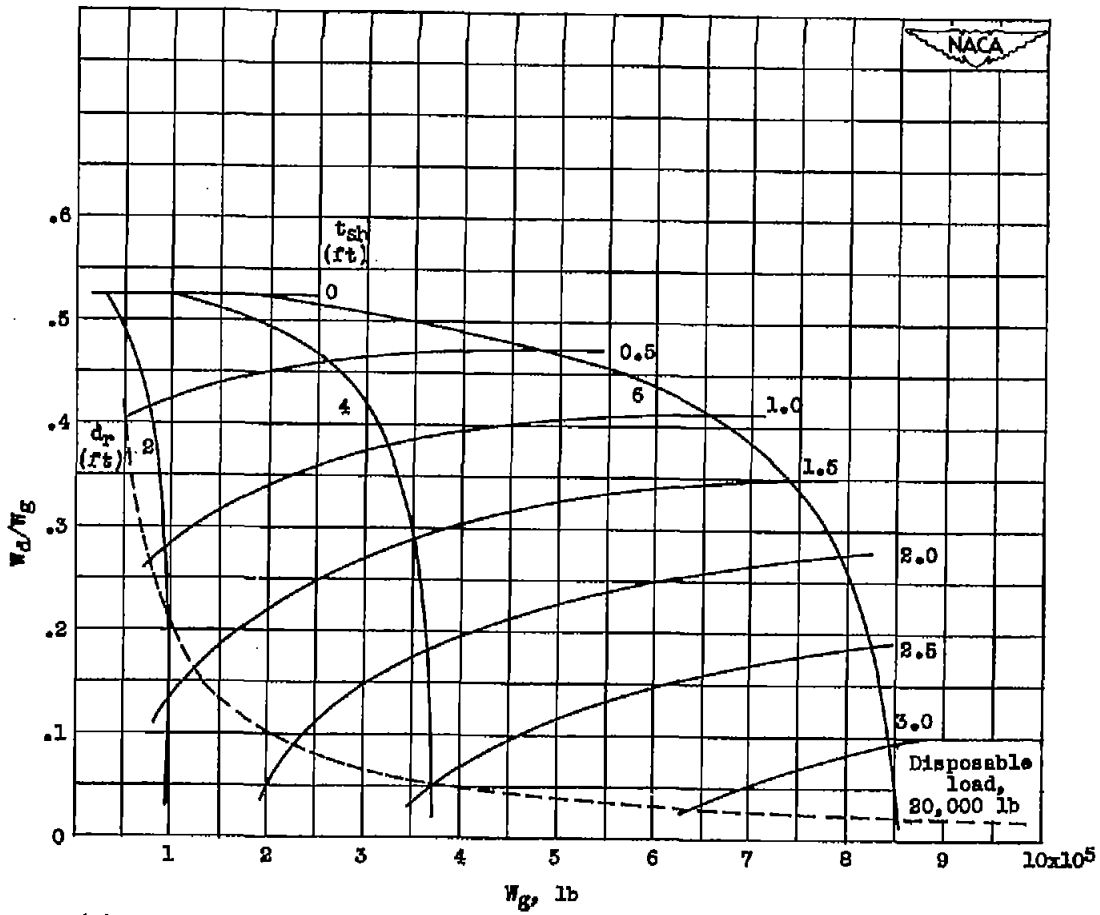

(c) Altitude, 30,000 feet; tube-wall temperature, 2000° R; turbine-inlet temperature, 1700° R; reactor free-flow-area ratio, 0.50.

Figure 12. - Continued. Variation of ratio of disposable load to airplane gross weight W_d/W_g with airplane gross weight W_g for various reactor diameters d_r and shielding thicknesses t_{sh}. Mass flow per unit reactor frontal area and compressor pressure ratio for maximum ratio of disposable load to airplane gross weight; flight Mach number, 0.9; reactor length, 2 feet; specific gravity of shielding, 6.0; lift-drag ratio, 18; airplane structural weight, 0.4 airplane gross weight.

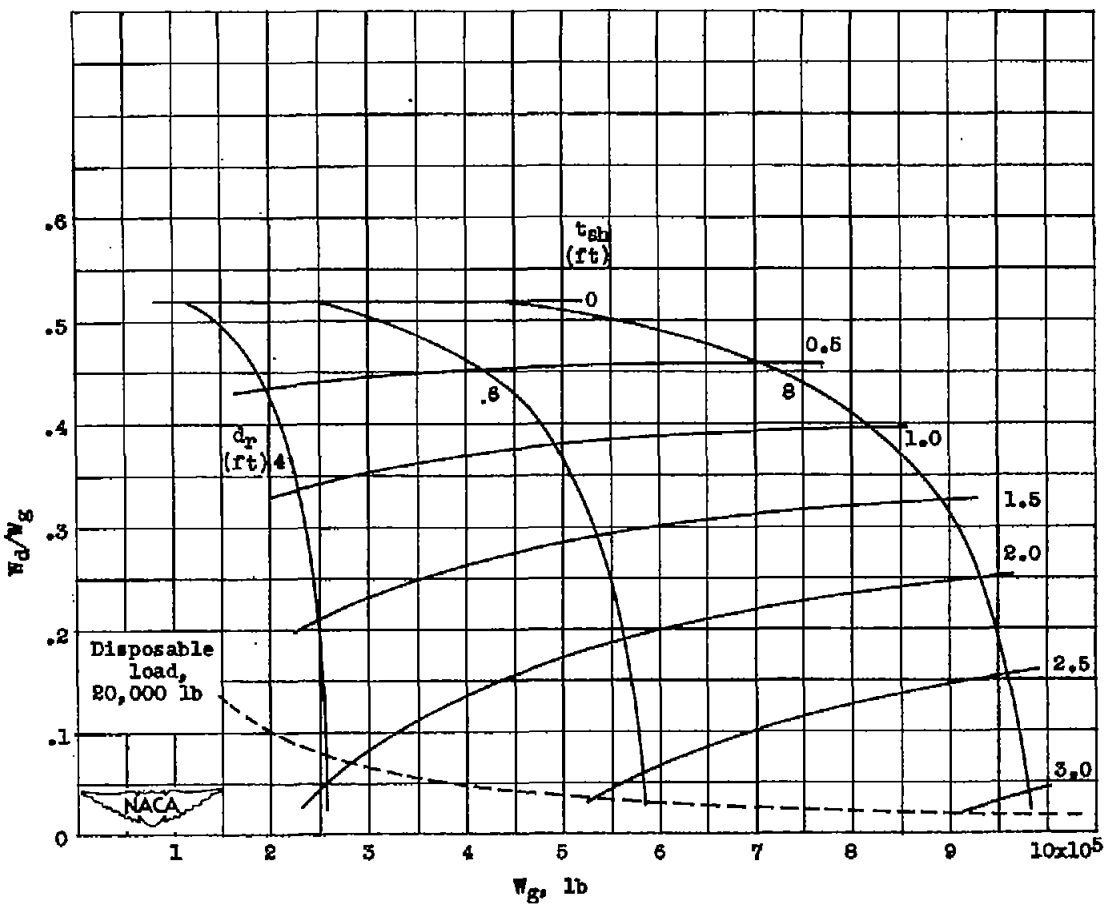

(d) Altitude, 30,000 feet; tube-wall temperature, 2000° R; turbine-inlet temperature, 1700° R; reactor free-flow-area ratio, 0.33.

Figure 12. - Continued. Variation of ratio of disposable load to airplane gross weight W_d/W_g with airplane gross weight W_g for various reactor diameters d_r and shielding thicknesses t_{sh}. Mass flow per unit reactor frontal area and compressor pressure ratio for maximum ratio of disposable load to airplane gross weight; flight Mach number, 0.9; reactor length, 2 feet; specific gravity of shielding, 6.0; lift-drag ratio, 18; airplane structural weight, 0.4 airplane gross weight.

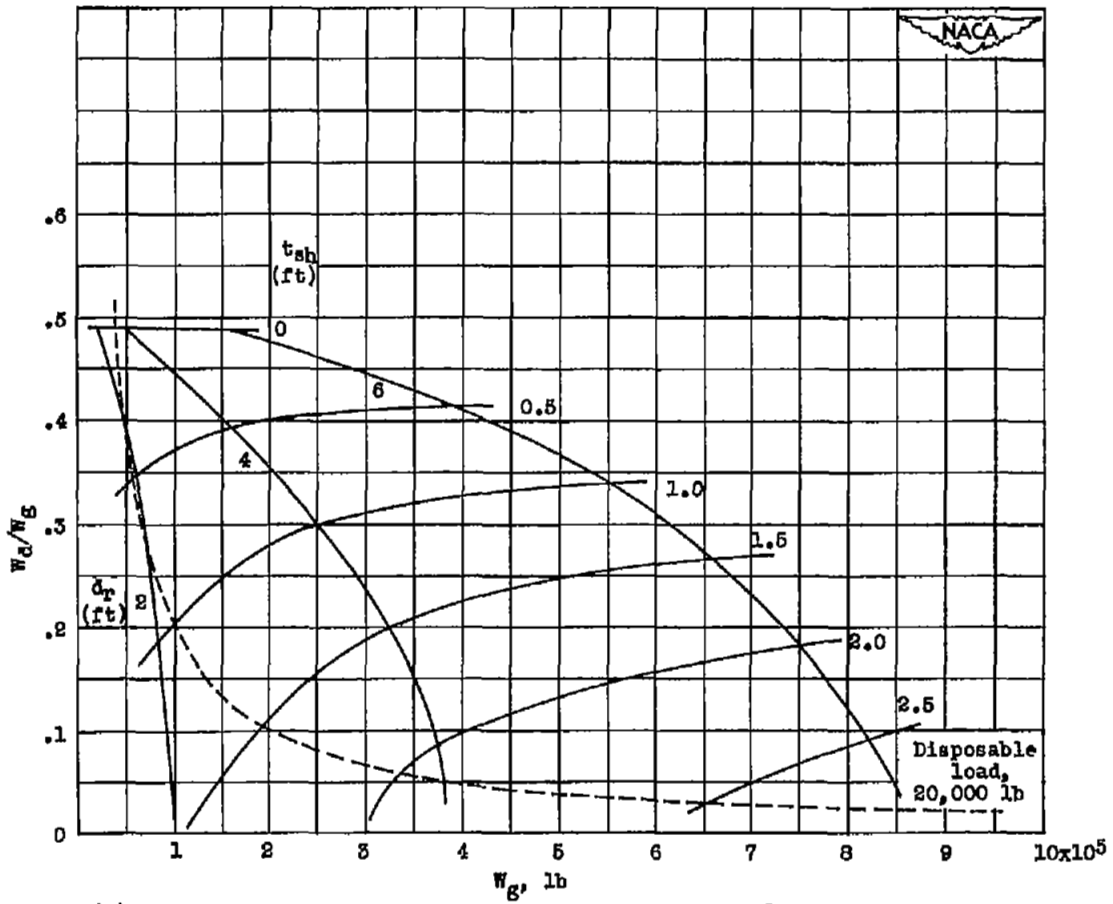

(e) Altitude, 50,000 feet; tube-wall temperature, 2500° R; turbine-inlet temperature, 2000° R; reactor free-flow-area ratio, 0.50.

Figure 12. - Continued. Variation of ratio of disposable load to airplane gross weight W_d/W_g with airplane gross weight W_g for various reactor diameters d_r and shielding thicknesses t_{sh}. Mass flow per unit reactor frontal area and compressor pressure ratio for maximum ratio of disposable load to airplane gross weight; flight Mach number, 0.9; reactor length, 2 feet; specific gravity of shielding, 6.0; lift-drag ratio, 18; airplane structural weight, 0.4 airplane gross weight.

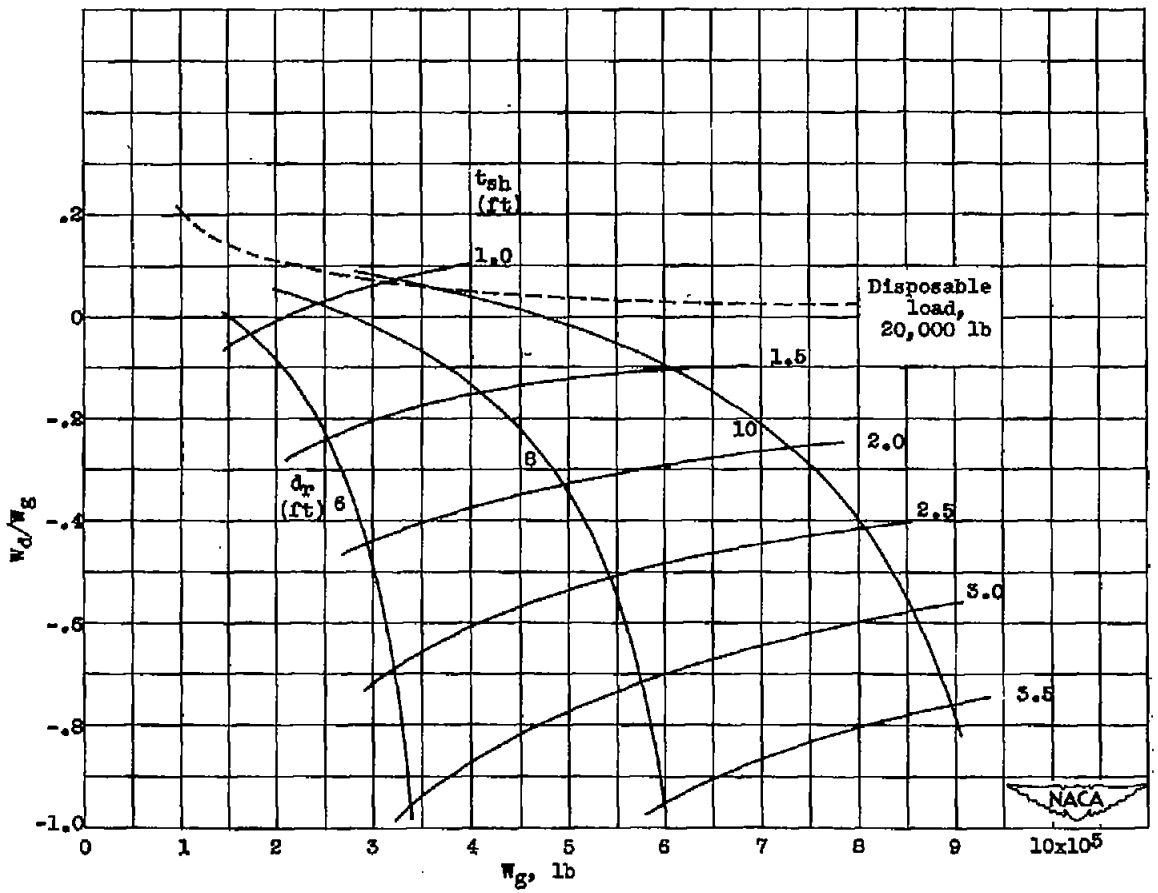

(f) Altitude, 70,000 feet; tube-wall temperature, 2500° R; turbine-inlet temperature, 2000° R; reactor free-flow-area ratio, 0.50.

Figure 12. - Concluded. Variation of ratio of disposable load to airplane gross weight W_d/W_g with airplane gross weight W_g for various reactor diameters d_r and shielding thicknesses t_{sh}. Mass flow per unit reactor frontal area and compressor pressure ratio for maximum ratio of disposable load to airplane gross weight; flight Mach number, 0.9; reactor length, 2 feet; specific gravity of shielding, 6.0; lift-drag ratio, 18; airplane structural weight, 0.4 airplane gross weight.

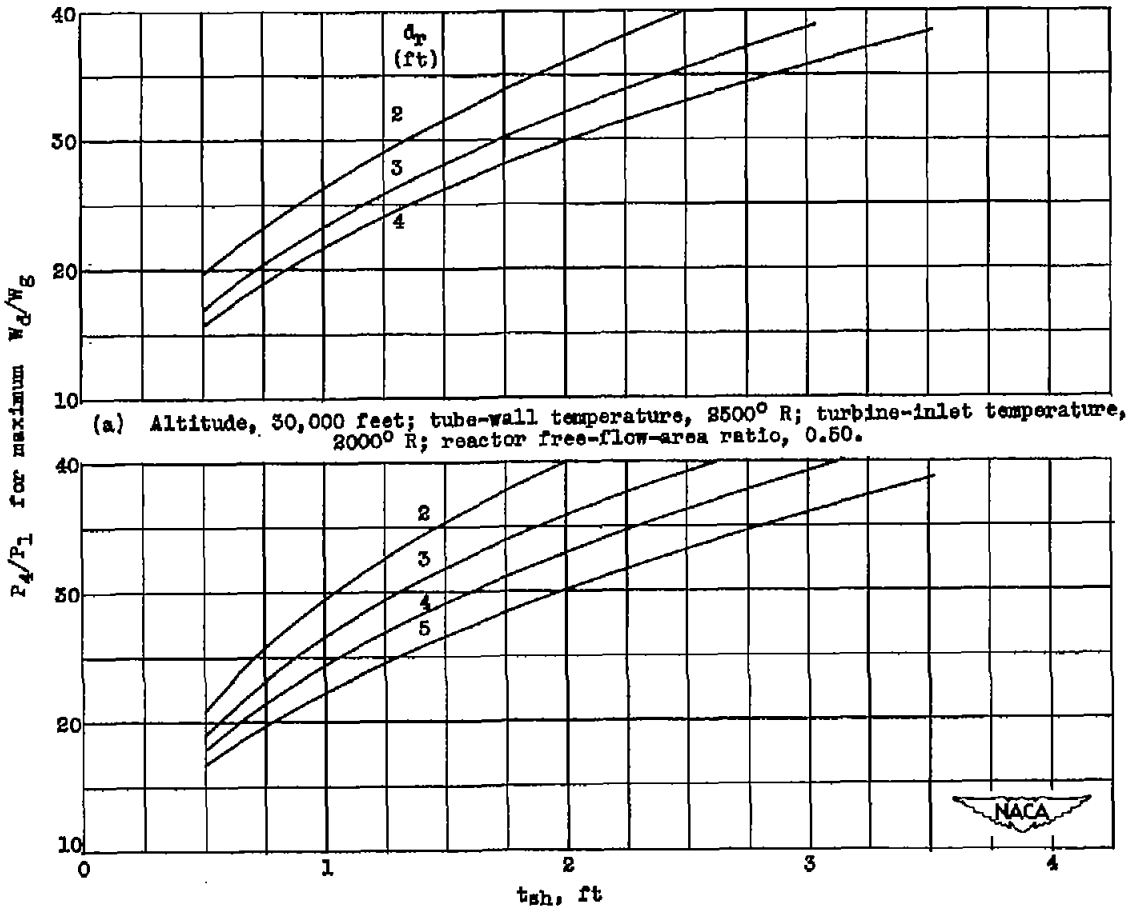

(a) Altitude, 30,000 feet; tube-wall temperature, 2500° R; turbine-inlet temperature, 2000° R; reactor free-flow-area ratio, 0.50.

(b) Altitude, 30,000 feet; tube-wall temperature, 2500° R; turbine-inlet temperature, 2000° R; reactor free-flow-area ratio, 0.33.

Figure 13. - Variation of compressor pressure ratio P_4/P_1 for maximum ratio of disposable load to airplane gross weight W_d/W_g with shielding thickness t_{sh} for various reactor diameters d_r. Mass flow per unit reactor frontal area for maximum ratio of disposable load to airplane gross weight; flight Mach number, 0.9; reactor length, 2 feet; specific gravity of shielding, 6.0; lift-drag ratio, 18; airplane structural weight, 0.4 airplane gross weight.

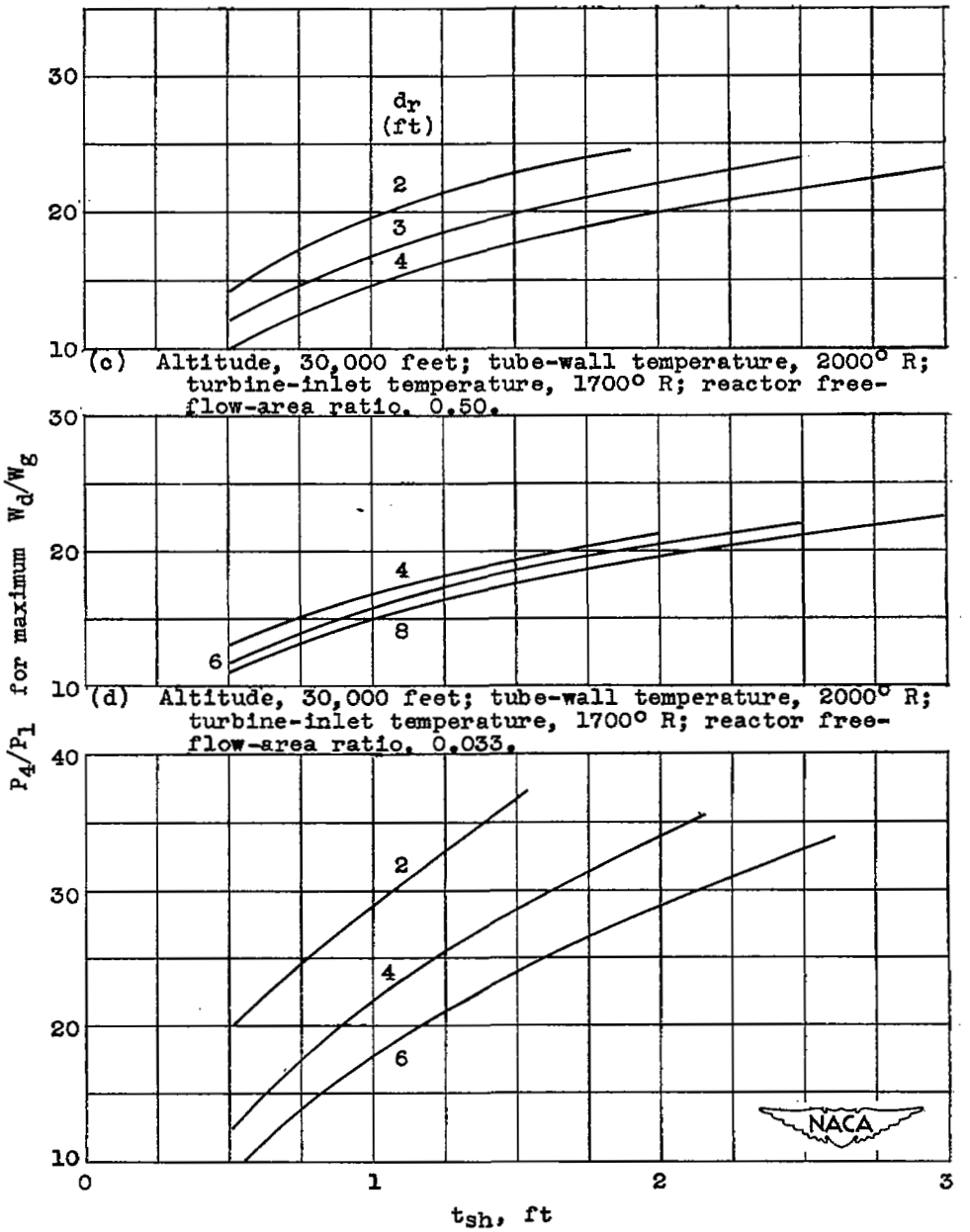

(c) Altitude, 30,000 feet; tube-wall temperature, 2000° R; turbine-inlet temperature, 1700° R; reactor free-flow-area ratio, 0.50.

(d) Altitude, 30,000 feet; tube-wall temperature, 2000° R; turbine-inlet temperature, 1700° R; reactor free-flow-area ratio, 0.033.

(e) Altitude, 50,000 feet; tube-wall temperature, 2500° R; turbine-inlet temperature, 2000° R; reactor free-flow-area ratio, 0.50.

Figure 13. - Concluded. Variation of compressor pressure ratio P_4/P_1 for maximum ratio of disposable load to airplane gross weight W_d/W_g with shielding thickness t_{sh} for various reactor diameters d_r. Mass flow per unit reactor frontal area for maximum ratio of disposable load to airplane gross weight; flight Mach number, 0.9; reactor length, 2 feet; specific gravity of shielding, 6.0; lift-drag ratio, 18; airplane structural weight, 0.4 airplane gross weight.

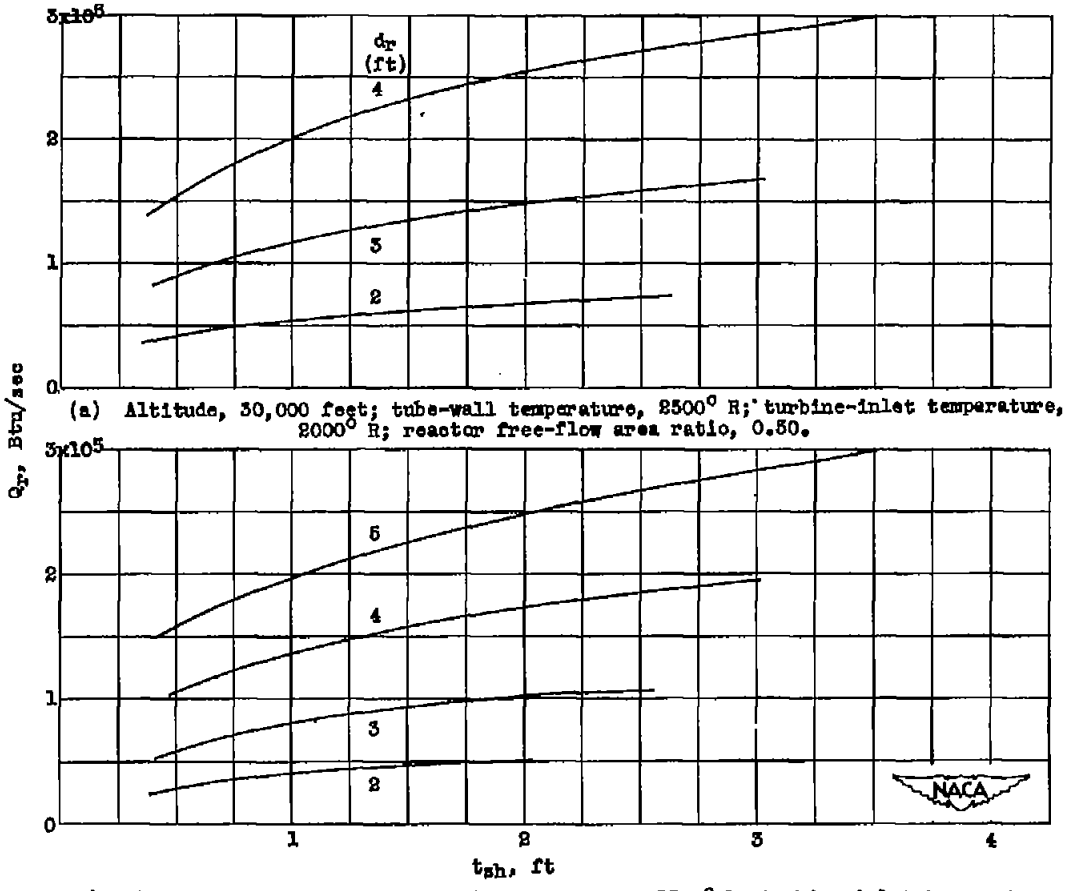

(a) Altitude, 30,000 feet; tube-wall temperature, 2500° R; turbine-inlet temperature, 2000° R; reactor free-flow area ratio, 0.50.

(b) Altitude, 30,000 feet; tube-wall temperature, 2500° R; turbine-inlet temperature, 2000° R; reactor free-flow area ratio, 0.33.

Figure 14. - Variation of reactor output Q_r with shielding thickness t_{sh} for various reactor diameters d_r. Mass flow per unit reactor frontal area and compressor pressure ratio for maximum ratio of disposable load to airplane gross weight; flight Mach number, 0.9; reactor length, 2 feet; specific gravity of shielding, 8.0; lift-drag ratio, 18; airplane structural weight, 0.4 airplane gross weight.

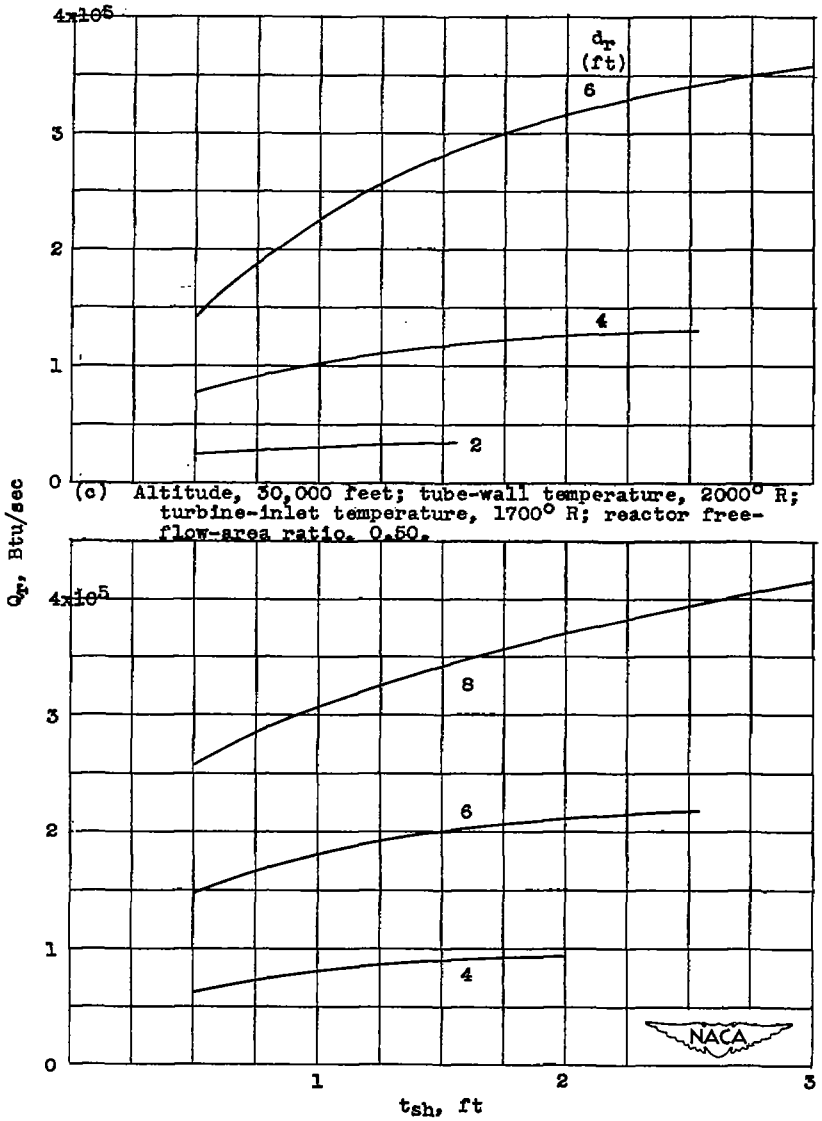

(c) Altitude, 30,000 feet; tube-wall temperature, 2000° R; turbine-inlet temperature, 1700° R; reactor free-flow-area ratio, 0.50.

(d) Altitude, 30,000 feet; tube-wall temperature, 2000° R; turbine-inlet temperature, 1700° R; reactor free-flow-area ratio, 0.33.

Figure 14. - Continued. Variation of reactor output Q_r with shielding thickness t_{sh} for various reactor diameters d_r. Mass flow per unit reactor frontal area and compressor pressure ratio for maximum ratio of disposable load to airplane gross weight; flight Mach number, 0.9; reactor length, 2 feet; specific gravity of shielding, 6.0; lift-drag ratio, 18; airplane structural weight, 0.4 airplane gross weight.

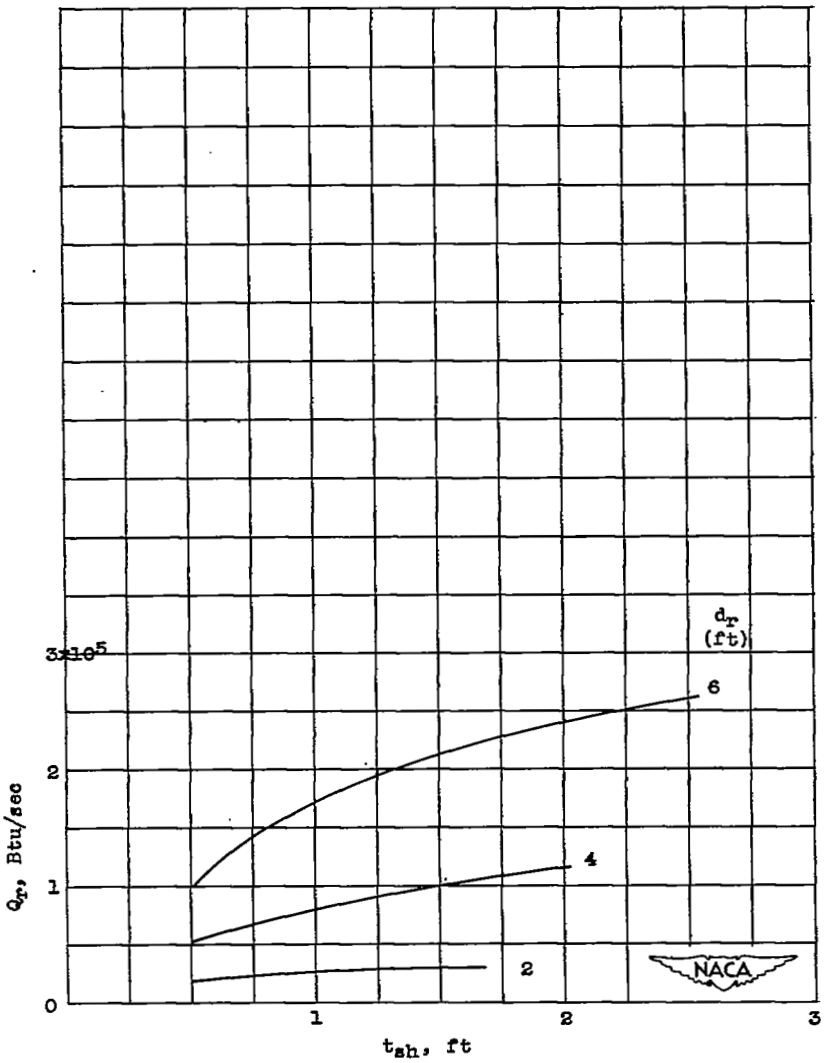

(e) Altitude, 50,000 feet; tube-wall temperature, 2500° R; turbine-inlet temperature, 2000° R; reactor free-flow area ratio, 0.50.

Figure 14. - Concluded. Variation of reactor output Q_r with shielding thickness t_{sh} for various reactor diameters d_r. Mass flow per unit reactor frontal area and compressor pressure ratio for maximum ratio of disposable load to airplane gross weight; flight Mach number, 0.9; reactor length, 2 feet; specific gravity of shielding, 6.0; lift-drag ratio, 18; airplane structural weight, 0.4 airplane gross weight.

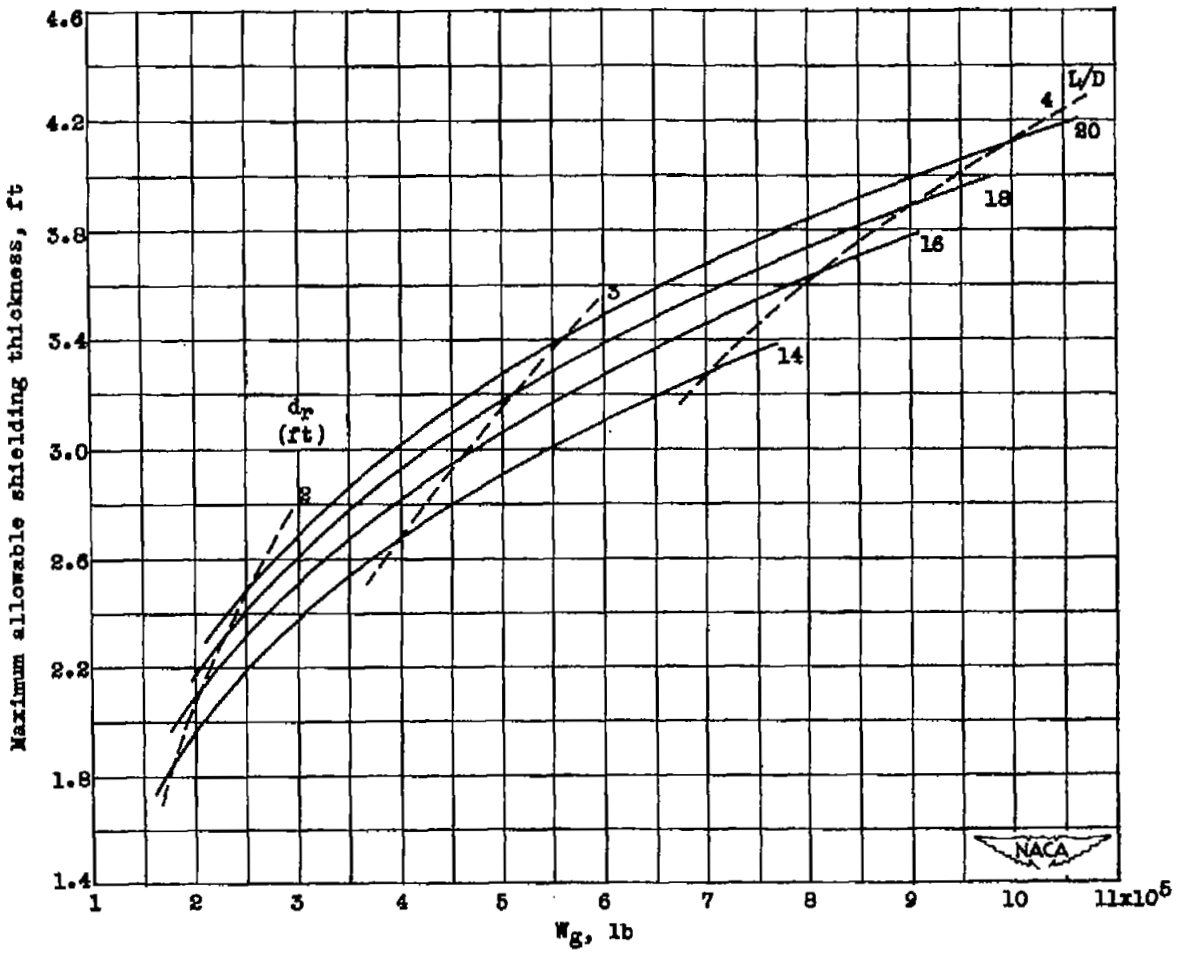

Figure 15. - Variation of maximum allowable shielding thickness with airplane gross weight W_g for various reactor diameters d_r and airplane (without nacelles) lift-drag ratios L/D. Mass flow per unit reactor frontal area and compressor pressure ratio for maximum allowable shielding thickness; flight Mach number, 0.9; altitude, 50,000 feet; tube-wall temperature, 2500° R; turbine-inlet temperature, 2000° R; reactor free-flow area ratio, 0.50; reactor length, 2 feet; specific gravity of shielding, 6.0; airplane structural weight, 0.4 airplane gross weight; disposable load, 20,000 pounds.

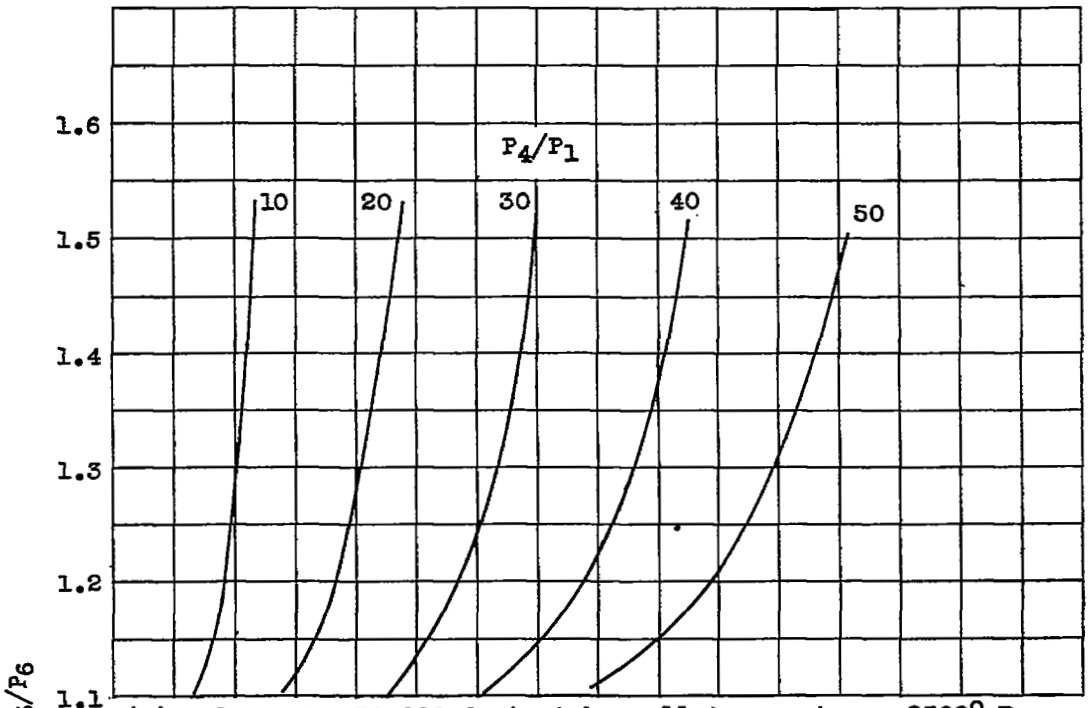

(a) Altitude, 30,000 feet; tube-wall temperature, 2500° R; turbine-inlet temperature, 2000° R; reactor free-flow-area ratio, 0.50.

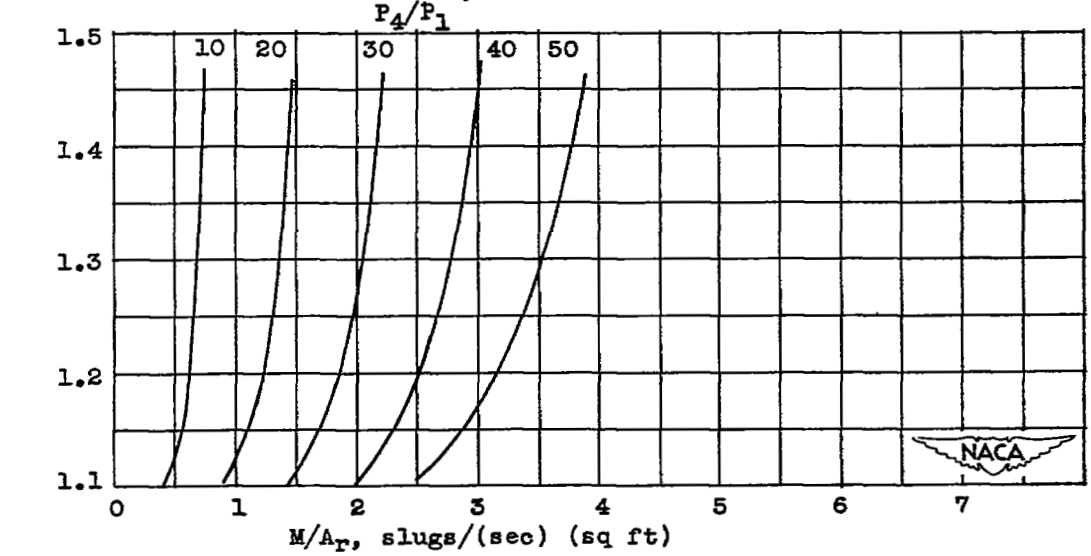

(b) Altitude, 30,000 feet; tube-wall temperature, 2500° R; turbine-inlet temperature, 2000° R; reactor free-flow-area ratio, 0.33.

Figure 16. - Variation of total-pressure ratio across reactor P_5/P_6 with mass flow per unit reactor frontal area M/A_r for various compressor pressure ratios P_4/P_1. Flight Mach number, 0.9.

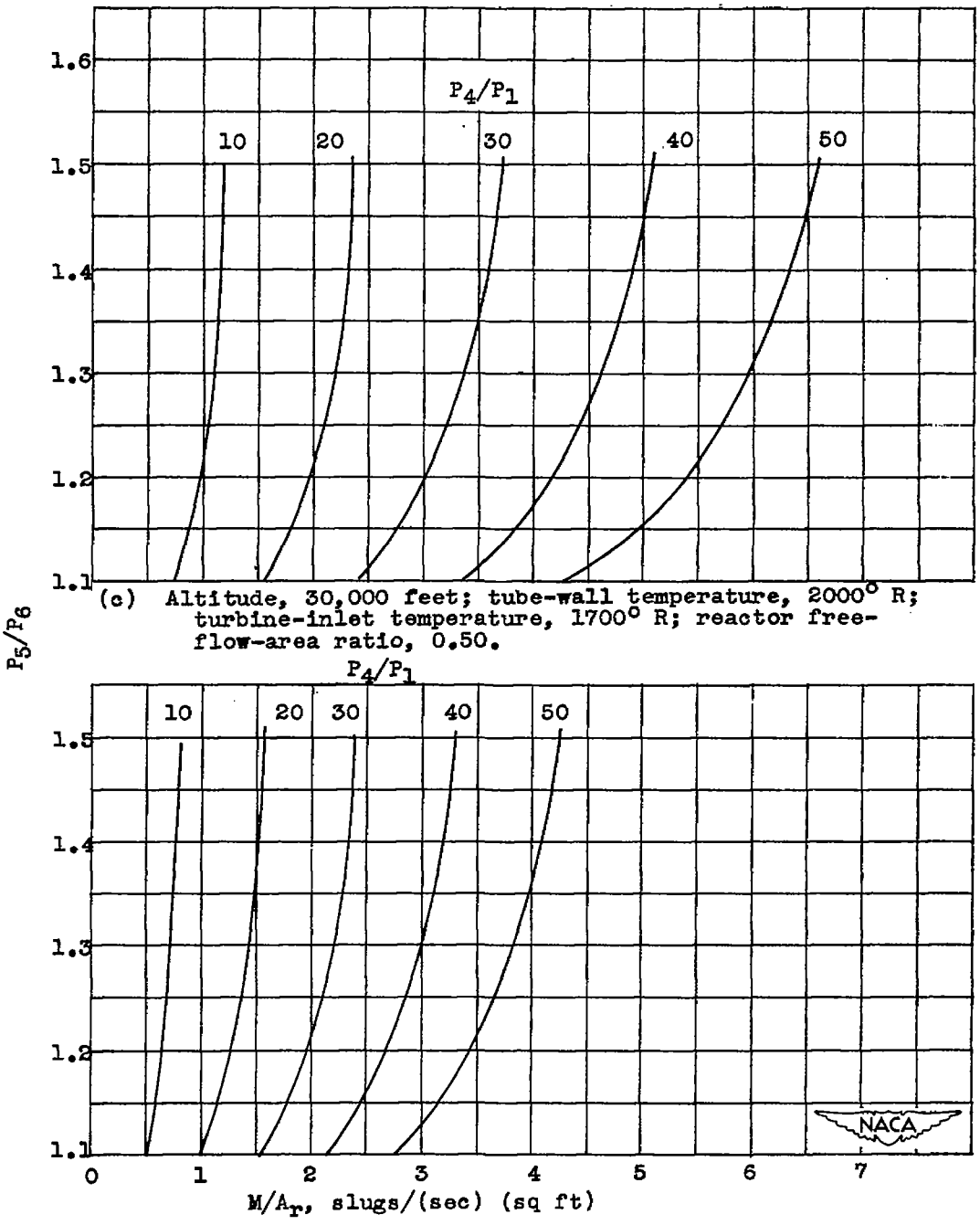

(c) Altitude, 30,000 feet; tube-wall temperature, 2000° R; turbine-inlet temperature, 1700° R; reactor free-flow-area ratio, 0.50.

(d) Altitude, 30,000 feet; tube-wall temperature, 2000° R; turbine-inlet temperature, 1700° R; reactor free-flow-area ratio, 0.33.

Figure 16. - Continued. Variation of total-pressure ratio across reactor P_5/P_6 with mass flow per unit reactor frontal area M/A_r for various compressor pressure ratios P_4/P_1. Flight Mach number, 0.9.

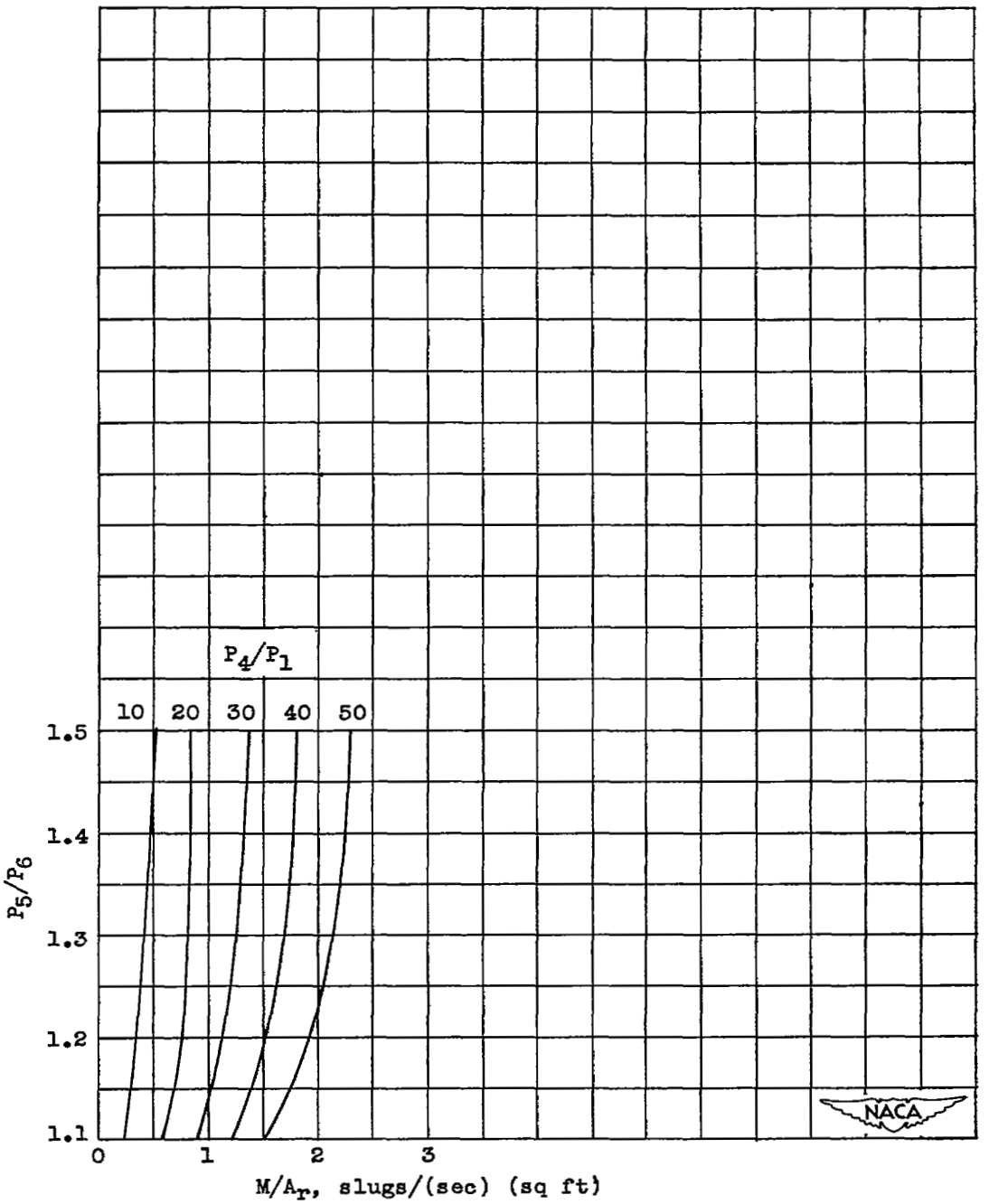

(e) Altitude, 50,000 feet; tube-wall temperature, 2500° R; turbine-inlet temperature, 2000° R; reactor free-flow-area ratio, 0.50.

Figure 16. - Concluded. Variation of total-pressure ratio across reactor P_5/P_6 with mass flow per unit reactor frontal area M/A_r for various compressor pressure ratios P_4/P_1. Flight Mach number, 0.9.